Available online at www.sciencedirect.com
SCIENCE DIRECT®
Biochemical and Biophysical Research Communications 310 (2003) 824–829
BBRC
www.elsevier.com/locate/ybbrc

Transcription factor Nrf2 is required for the constitutive and inducible expression of multidrug resistance-associated protein 1 in mouse embryo fibroblasts

Asako Hayashi,[a] Hiroshi Suzuki,[a] Ken Itoh,[b] Masayuki Yamamoto,[b] and Yuichi Sugiyama[a,*]

[a] *School of Pharmaceutical Sciences, The University of Tokyo, Hongo, Bunkyo-ku, Tokyo 113-0033, Japan*
[b] *Center for Tsukuba Advanced Research Alliance and Institute of Basic Medical Sciences, University of Tsukuba, Tennoudai, Tsukuba 305-8577, Japan*

Received 29 July 2003

Abstract

The nuclear factor-E2 p45-related factor (Nrf) 2 is a transcription factor for the antioxidant responsive element-mediated induction of enzymes responsible for conjugation. Since multidrug resistance-associated protein1 (Mrp1/Abcc1) is an ATP-binding cassette transporter which plays an important role in the cellular extrusion of conjugated metabolites and, therefore, acts synergistically with conjugating enzymes for the cellular detoxification of xenobiotics, we examined the possibility that Nrf2 is also involved in the expression of Mrp1 in mouse embryo fibroblasts. The constitutive expression levels of Mrp1 mRNA and protein were significantly lower in Nrf2 (−/−) cells compared with those in wild type cells. In addition, significant induction by diethyl maleate was observed in wild type, but not in Nrf2 (−/−), cells, suggesting the involvement of Nrf2 in both the constitutive and inducible mRNA and protein expression of Mrp1. In addition, the uptake of [^{3}H]2,4-dinitrophenyl-*S*-glutathione, a typical substrate of Mrp1, into isolated membrane vesicles also demonstrated that Nrf2 regulates the transport activity of glutathione conjugates in mouse fibroblasts. This is the first demonstration that Nrf2 is required for the constitutive and inducible expression of Mrp family proteins.

Keywords: Nrf2; Mrp1; Induction; Oxidative stress

It has been suggested that the metabolizing enzymes and efflux transporters act synergistically in the detoxification of xenobiotics [1]. Among them, conjugation of xenobiotics with glutathione (GSH), followed by the cellular extrusion of GSH-conjugates, has been reported to be essential for the survival of many kinds of organisms including bacteria, yeasts, plants, and mammals [1]. In mammals, such a synergistic role has been reported for glucuronidation and sulfation followed by cellular extrusion in somatic cells such as hepatocytes and enterocytes [2–4].

The detoxification pathway via GSH-conjugation has been studied extensively. GSH *S*-transferases (GSTs) play an important role in the conjugation of xenobiotics with GSH, whose synthesis is rate determined by γ-glutamylcysteinyl synthetase (γ-GCS). It has been suggested that the enzymes which are responsible for the formation of GSH-conjugates (γ-GCS and GSTs) and multidrug resistance associated protein (MRP/ABCC) family proteins, responsible for the cellular extrusion of GSH-conjugates, are coordinately induced under certain conditions [5–7]. For example, in cisplatin-resistant HL-60 cells originating from human leukemia, the expression of both γ-GCS and MRP1/ABCC1 is induced [5]. In addition, there is a correlation in the expression level of MRP1 and γ-GCS in dissected human colon tumor specimens [6]. Such a correlation has also been reported for many kinds of tumor cells which have acquired drug resistance.

Concerning the mechanism for the induction of GSTs and γ-GCS, it has been shown that the basic-region leucine-zipper factor Nuclear factor-erythroid 2 p45-related factor 2 (Nrf2) is essential for antioxidant

* Corresponding author. Fax: +81-3-5841-4766.
E-mail address: sugiyama@mol.f.u-tokyo.ac.jp (Y. Sugiyama).

0006-291X/$ - see front matter © 2003 Elsevier Inc. All rights reserved.
doi:10.1016/j.bbrc.2003.09.086

responsive element (ARE)-mediated induction [8,9]. In mice with targeted disruption of Nrf2, reductions have been reported in the constitutive and/or inducible expression of class Alpha, class Mu, and class Pi GSTs, and the heavy subunit of γ-GCS (γ-GCS-h) [8,10–16]. In addition, it was recently demonstrated that the expression of xCT, a component of system Xc−, which is responsible for cystine/glutamate exchange and consequently for maintaining the intracellular GSH concentration, is also under the control of Nrf2 [17]. In contrast, the molecular mechanism for the induction of MRP1 has not been clarified, although it has been revealed that MRP1 is induced by antioxidants such as *t*-butylhydroquinone (*t*BHQ) and quercetin in HepG2 and MCF-7 cells originating from human breast cancer [18]. In the present study, we carried out an investigation to see whether Nrf2 is required for the constitutive and inducible expression of Mrp1 by using embryo fibroblasts derived from control and Nrf2 (−/−) mice [17].

Materials and methods

Materials. Unlabeled and [^{3}H]labeled 2,4-dinitrophenyl-*S*-glutathione (DNP-SG; 50 μCi/nmol) were synthesized enzymatically with unlabeled and [glycine-2-^{3}H]GSH (NEN Life Sciences), 1-chloro-2,4-dinitrobenzene, and GST (Sigma Chemical, St. Louis, MO) as described previously [19]. Monoclonal anti-Mrp1 antibody (MRPr1) was purchased from Alexis Biochemicals (San Diego, CA). All other chemicals used were commercially available and of reagent grade.

Mouse embryo fibroblasts, prepared either from wild type or Nrf2 knockout mice [17], were cultured in Iscove's modified Dulbecco's medium supplemented with 10% fetal bovine serum, 10 ng/ml human recombinant epidermal growth factor, 1× insulin-transferrin-selenium-G supplement, and 10% penicillin-streptomycin (Invitrogen) at 37 °C in 5% CO_2 and 95% air.

Quantification of mRNA expression levels by real time PCR. Total RNA was isolated using Isogen (Nippon Gene, Toyama, Japan). mRNA was isolated from total RNA using Oligotex-dT30 (Roche Diagnostics, Basel, Switzerland). mRNA (0.4 μg) was reverse transcribed using the One Step RNA PCR kit (AMV; Takara, Shiga, Japan) according to the manufacturer's instructions. mRNA expression levels of Mrp1, GST-Pi, and γ-GCS-h in relation to that of GAPDH were determined in the Light Cycler System (Roche Diagnostics, Basel, Switzerland). PCRs were performed according to the manufacturer's instructions with 0.5 μM each of the respective forward and reverse primers (Table 1) and 2× QuantiTect SYBR Green PCR Master Mix (QuantiTect SYBR Green PCR kit (Qiagen, Hilden, Germany) in a total volume of 20 μL. Conditions for amplification were as follows: 10 min at 95 °C, followed by 45 cycles with 15 s at 95 °C, 25 s at the indicated annealing temperatures (Table 1) and 20 s at 72 °C. The quantity of GAPDH, Mrp1, GST-Pi, and γ GCS-h was determined using a serial plasmid DNA dilution from 10^{-5} to 1 pg as the amplification standard. Melting curve analysis and electrophoretic analysis of the amplification products revealed that only one cDNA fragment was detected in each target transporter, and that this fragment had the size expected from the known cDNA sequence of the respective transporter.

Preparation of membrane vesicles. All steps were performed at 0–4 °C. Mouse embryo fibroblasts were washed and scraped into phosphate-buffered saline and washed by centrifugation (4000*g* for 10 min). The pellet was stored at −80 °C until required. Then the membrane vesicles were prepared according to the method described previously [19]. The isolated membrane vesicles were frozen in liquid nitrogen and stored at −80 °C until required. Protein concentrations were determined by the Lowry method using bovine serum albumin as a standard.

Western blotting. For the Western blot analysis, 10 μg crude membrane was dissolved in 3× SDS sample buffer (New England BioLabs, Beverly, MA) and subjected to electrophoresis on a 7% SDS–polyacrylamide gel with a 4.4% stacking gel. The molecular weight was determined using a prestained protein marker (New England BioLabs, Beverly, MA). Proteins were transferred electrophoretically to a nitrocellulose membrane (Millipore, Bedford, MA) using a blotter (Bio-Rad Laboratories, Richmond, CA) at 15 V for 1 h. The membrane was blocked with Tris-buffered saline containing 0.05% Tween 20 (TBS-T) and 5% skimmed milk powder at 4 °C for overnight. After washing with TBS-T, the membrane was incubated for 1 h at room temperature in TBS-T containing 100-fold diluted anti-Mrp1 antibody (MRPr1). The membrane was allowed to bind to anti-rat IgG conjugated with horseradish peroxidase (Amersham Biosciences, Buckinghamshire, UK). The enzyme activity was assessed using the ECL Plus Western blotting Starter Kit (Amersham Biosciences) and a luminescence image analyzer (LAS-1000 plus, Fuji Film).

Transport study with membrane vesicles. Transport studies were performed using the rapid filtration technique described in a previous report [19]. Transport medium (10 mM Tris, 250 mM sucrose, and 10 mM $MgCl_2$, pH 7.4) containing 0.5 μM [^{3}H]DNP-SG (15 μl), with or without unlabeled substrate, was preincubated at 37 °C for 3 min and then rapidly mixed with 5 ml membrane vesicle suspension (10 μg of protein), with or without 5 mM ATP and ATP-regenerating system (10 mM creatine phosphate, and 100 μg/ml creatine phosphokinase). To check the ATP dependence, ATP was replaced by AMP. The transport reaction was stopped by adding 1 ml ice-cold buffer containing 250 mM sucrose, 0.1 M NaCl, and 10 mM Tris–HCl (pH 7.4). The stopped reaction mixture was filtered through a 0.45 μm HA filter (Millipore, Bedford, MA) and washed twice with 5 ml stop solution. Radioactivity retained on the filter was determined using a liquid scintillation counter (LSC-3500, Aloka, Tokyo, Japan).

Table 1
Oligonucleotide primers and annealing temperature for the real time PCR

mRNA	Primers	Annealing temperature (°C)
Mrp1	Forward: 5′-dACCTGCGCTTCAAGATCACC-3′ Reverse: 5′-dCACAGTCGGAACGGACTGTT-3′	57
GST-Pi	Forward: 5′-dGTGTGAGGCCATGCGAATGC-3′ Reverse: 5′-dCGTCGAGGGGTTCAAACTCC-3′	60
γGCS-h	Forward: 5′-dCAAGGACGTGCTCAAGTGGG-3′ Reverse: 3′-dCCTGTTTGGGGTTGGTAGGC-5′	55
GAPDH	Forward: 5′-dCCAGTATGACTCCACTCACG-3′ Reverse: 3′-dGTGGTAGAAGGTCCTCGCTC-5′	57

Results

Involvement of Nrf2 in the expression of Mrp1 in mouse embryo fibroblasts

The amount of Mrp1 mRNA was compared in control and Nrf2 (−/−) fibroblasts by real time PCR under both constitutive and inducible conditions (Fig. 1A). We also examined the expression of GST-Pi (Fig. 1B) and γ-GCS-h (Fig. 1C) as the positive control, since the involvement of Nrf2 in the expression of these enzymes has been reported. Constitutive expression of Mrp1, GST-Pi, and γ-GCS-h was reduced in Nrf2 (−/−) fibroblasts to 38%, 51%, and 32% of that observed in the control fibroblasts, respectively (Fig. 1). Furthermore, although diethyl maleate (DEM), an antioxidant, increased the mRNA levels of Mrp1, GST-Pi, and γ-GCS-h by approximately 2–4-fold in the control fibroblasts, there was no induction of these mRNAs by DEM in Nrf2 (−/−) fibroblasts (Fig. 1).

Moreover, Western blotting revealed the involvement of Nrf2 in the protein expression of Mrp1 in mouse embryo fibroblasts. Constitutive expression of Mrp1 in Nrf2 (−/−) fibroblasts was reduced to 32% of that in the control fibroblasts, and the approximately 1.6-fold induction by DEM in the control fibroblasts was absent in Nrf2 (−/−) fibroblasts (Fig. 2).

Transport studies with membrane vesicles prepared from fibroblasts

We examined whether the transport function is also under the control of Nrf2. Isolated membrane vesicles were used for this purpose. Fig. 3 shows the time-profiles for the uptake of [^{3}H]DNP-SG, an Mrp1 substrate, into isolated membrane vesicles from wild type

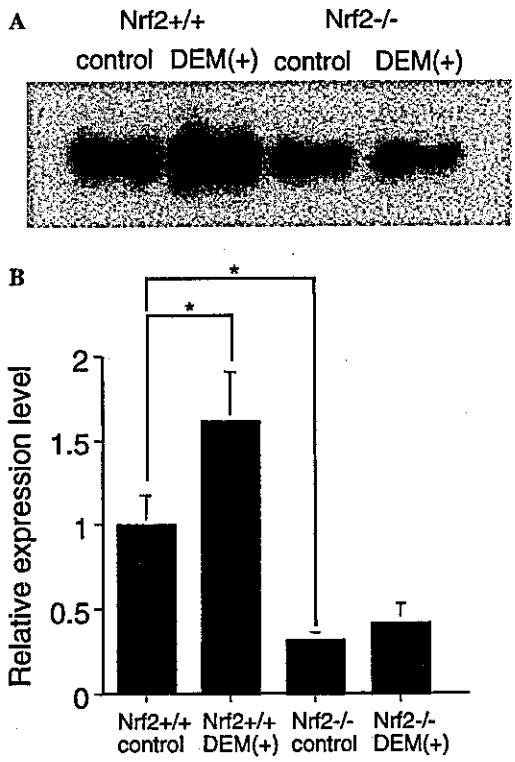

Fig. 2. Effect of DEM on the expression of Mrp1 protein. The cells were incubated for 6 h with or without 100 μM DEM. Membrane vesicles were prepared and the expression level was compared in control and Nrf2 (−/−) fibroblasts by Western blot analysis. Five microgram aliquots of proteins were loaded and separated on a 7% polyacrylamide gel containing 0.1% SDS. The fractionated proteins were transferred to the membrane filter by electroblotting and Mrp1 was detected by monoclonal anti-Mrp1 antibody (MRPr1). A typical result is shown in panel (A) and the result of quantification is shown in panel (B). Protein expression levels are expressed as a ratio with respect to vehicle-treated wild-type controls. Data represent means ± SE of two independent experiments performed in triplicate. $^{**}P < 0.01$, significantly different from vehicle-treated control cells.

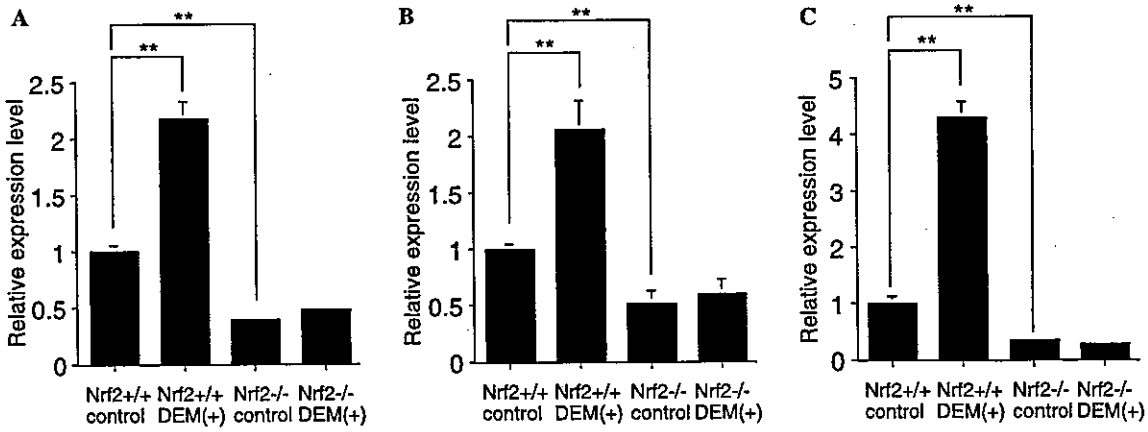

Fig. 1. Effect of DEM on the expression of Mrp1, GST-Pi, and γ-GCS-h mRNAs. The control and Nrf 2 (−/−) fibroblasts were incubated for 6 h with or without 100 μM DEM. The expression level of mRNA was compared in control and Nrf2 (−/−) fibroblasts by the real time PCR. Levels of Mrp1 (A), GST-Pi (B), and γ-GCS-h (C) mRNA were normalized to GAPDH mRNA levels and expressed as a ratio with respect to vehicle-treated wild-type controls. Data represent means ± SE of two independent experiments performed in triplicate. $^{**}P < 0.01$, significantly different from the vehicle-treated control cells.

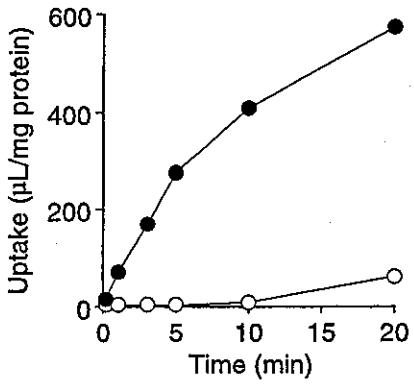

Fig. 3. Time-profiles of the uptake of [^{3}H]DNP-SG into isolated membrane vesicles from fibroblasts. Membrane vesicles (10 μg of protein) prepared from fibroblasts were incubated in the medium containing [^{3}H]DNP-SG (0.5 μM) at 37 °C in the presence (●) and absence (○) of 5 mM ATP and ATP-regenerating system (10 mM creatine phosphate and 100 μg/ml creatine phosphokinase). Each point represent the mean ± SE of three independent determinations.

fibroblasts in the presence or absence of ATP. ATP significantly stimulates the uptake of [^{3}H]DNP-SG (Fig. 3). The ATP-dependent uptake was linear up to 5 min (Fig. 3). Fig. 4 shows the comparison of the ATP-dependent uptake for 3 min into membrane vesicles prepared from control and Nrf2 (−/−) fibroblasts. The effect of DEM was also examined (Fig. 4). The uptake of [^{3}H]DNP-SG into membrane vesicles prepared from Nrf2 (−/−) fibroblasts was approximately 50% of that from the control fibroblasts (Fig. 4). Treatment of the wild type fibroblasts with DEM resulted in an approximately 1.4-fold increase in the uptake of [^{3}H]DNP-SG by membrane vesicles (Fig. 4). In addition, treatment of Nrf2 (−/−) fibroblasts with DEM also resulted in an increase in the uptake of [^{3}H]DNP-SG into isolated membrane vesicles (Fig. 4).

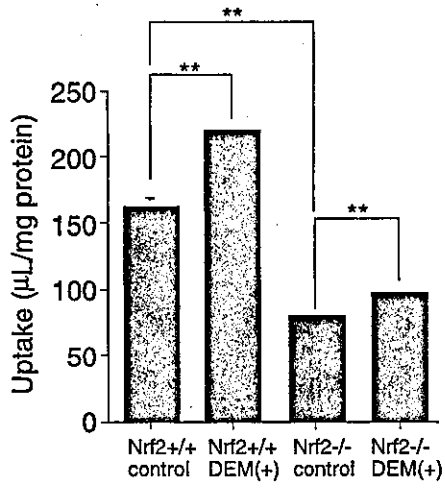

Fig. 4. Effect of DEM on the uptake of [^{3}H]DNP-SG into isolated membrane vesicles from fibroblasts. Membrane vesicles (10 μg of protein) prepared from fibroblasts were incubated in the medium containing [^{3}H]DNP-SG (0.5 μM) at 37 °C for 3 min in the presence and absence of 5 mM ATP and ATP-regenerating system (10 mM creatine phosphate and 100 μg/ml creatine phosphokinase). The results show ATP-dependent uptake. Data represent means ± SE of two independent experiments performed in triplicate. **$P < 0.01$, significant difference between the two comparisons.

Discussion

The purpose of the present study was to investigate the involvement of Nrf2 in the expression of Mrp1. Using embryo fibroblasts prepared from control and Nrf 2 (−/−) mice, we compared the mRNA and protein levels of Mrp1 (Figs. 1 and 2). Initially, we quantified the mRNA expression levels of Mrp1 by real time PCR using a Light Cycler. The constitutive mRNA expression of Mrp1 was significantly lower in fibroblasts prepared from Nrf2 (−/−) mice compared with wild type fibroblasts (Fig. 1). Furthermore, DEM increased the mRNA levels of Mrp1 only in the control fibroblasts and the induction was not seen in Nrf2 (−/−) fibroblasts (Fig. 1). Northern blot analysis and semi-quantitative RT-PCR provided similar data (not shown). The results of the Western blot analysis also indicated that Nrf2 is involved in both the constitutive expression and induction of Mrp1 protein (Fig. 2). It was thus suggested that Nrf2 is involved in both constitutive and inducible mRNA and protein expression of Mrp1. The fact that the expression of Mrp1 is still observed in Nrf2 (−/−) fibroblasts (Figs. 1 and 2) may be accounted for by assuming that AP-1, which also binds to the consensus sequence for Nrf2, may compensate for the loss of Nrf2 [20]. This is the first demonstration to show that Nrf2 is required for the constitutive and inducible expression of an efflux transporter.

The results were further confirmed by examining the function of Mrp1. For this purpose, we investigated the ATP-dependent transport of an Mrp1 substrate, DNP-SG, in isolated membrane vesicles. The uptake of [^{3}H]DNP-SG into membrane vesicles prepared from Nrf2 (−/−) fibroblasts was approximately 50% of that from the control fibroblasts (Fig. 4), which is consistent with the results of the Western blot analysis (Fig. 2). In addition, DEM treatment increased the uptake of [^{3}H]DNP-SG into membrane vesicles prepared from the control fibroblasts (Fig. 4), which is also supported by the induction of Mrp1 demonstrated by Western blot analysis (Fig. 2). However, significant induction of transport activity by DEM was also observed even in membrane vesicles from Nrf2 (−/−) fibroblasts (Fig. 4). Since the expression of Mrp1 protein is not induced by DEM in Nrf2 (−/−) fibroblasts, it is possible that some other transporter(s) which are not under the control of Nrf2 may be induced by DEM. Such an Nrf2-independent induction has also been reported for GST in Nrf2 (−/−) mice [10].

As a control for the regulation of Mrp1 gene expression, we examined the mRNA levels of γ-GCS-h and GST-Pi. As shown in Fig. 1, γ-GCS-h mRNA in Nrf2 (−/−) fibroblasts was reduced to 32% of that in control fibroblasts, which is consistent with the previous report [13]. The reduction of intracellular GSH levels in Nrf2 (−/−) cells compared with the control cells (3.0 vs. 5.7 nmol/mg protein; unpublished observations) may be accounted for by the reduced biosynthesis of GSH whose rate determining process is catalyzed by γ-GCS. In addition, we also confirmed that the expression of GST-Pi in Nrf2 (−/−) fibroblasts was approximately 50% of that in control fibroblasts, which is consistent with the previous finding that the expression of many GST isozymes is regulated by Nrf2 [16]. Consequently, together with the previous finding that xCT, a component of cystine/glutamate exchanger required for maintaining cellular GSH synthesis, is also regulated by Nrf2, suggests that all processes required for the detoxification of xenobiotics via the formation of GSH-conjugates (such as the synthesis of GSH, conjugation with GSH, and the cellular extrusion of GSH-conjugate) are regulated by Nrf2. The previous finding that the expression of γ-GCS and MRP1 is coordinately induced by oxidative stress [7] may be accounted for by considering that these two proteins are induced in an Nrf2-dependent manner.

In addition to the reduction of the formation of GSH-conjugates, the reduction in the cellular extrusion of GSH-conjugates via Mrp1 in Nrf2 (−/−) cells may be related to the increased sensitivity of Nrf2 (−/−) mice to carcinogens [15]. This hypothesis is based on the fact that, in general, the cellular concentrations of xenobiotics and their GSH-conjugates are in equilibrium and Mrp1 acts to reduce the cellular concentrations of xenobiotics by pumping out their GSH-conjugates and consequently shifting the equilibrium. The significant reduction of Mrp1 and GSH levels in Nrf2 (−/−) cells may also result in the increased sensitivity of the knockout mice to chemotherapeutic agents, since many kinds of chemotherapeutic agents (such as etoposide and daunomycin) are known to be co-transported with GSH via Mrp1/MRP1 [21,22]. Indeed, Mrp1 (−/−) mice are much more sensitive than the control mice against etoposide [23,24].

Finally, the role of Nrf2 in the constitutive and inducible expression of Mrp1 needs to be discussed in relation to the promoter sequence of this gene. It has been established that Nrf2 mediates the transcriptional activation of genes via an ARE [8,9]. The consensus ARE sequences such as 5′-ttgagttagct-3′ and 5′-ttgagac agca-3′ are located between nt −1240 and −1229, and between nt −2020 and −2010 of mouse Mrp1 gene, respectively. It is possible that Nrf2 may bind to these consensus sequences, although this remains to be clarified experimentally. Since ARE consensus sequences such as 5′-gtgactcagc-3′ and 5′-gtgacaaagca-3′ are also present between nt −499 and −490, and between nt −1843 and −1833 in the 5′-flanking region of human MRP1, respectively, human MRP1 may also be under the control of Nrf2. This may be related to the induction of human MRP1 by *t*BHQ and quercetin in HepG2 and MCF-7 cells [18].

In conclusion, we found that Nrf2 is required for the constitutive and inducible expression of Mrp1. It was also suggested that the expression of Mrp1, an efflux transporter for GSH-conjugates, along with xCTG, γ-GCS, and GST, is also under the control of Nrf2. The results of the present study may provide the molecular basis for the coordinate induction of drug metabolizing enzymes and efflux transporter(s).

References

[1] T. Ishikawa, Z.S. Li, Y.P. Lu, P.A. Rea, The GS-X pump in plant, yeast, and animal cells: structure, function, and gene expression, Biosci. Rep. 17 (1997) 189–207.
[2] H. Suzuki, Y. Sugiyama, Role of metabolic enzymes and efflux transporters in the absorption of drugs from the small intestine, Eur. J. Pharm. Sci. 12 (2000) 3–12.
[3] H. Suzuki, Y. Sugiyama, Single nucleotide polymorphisms in multidrug resistance associated protein 2 (MRP2/ABCC2): its impact on drug disposition, Adv. Drug Deliv. Rev. 54 (2002) 1311–1331.
[4] D. Keppler, J. König, Hepatic secretion of conjugated drugs and endogenous substances, Semin. Liver Dis. 20 (2000) 265–272.
[5] T. Ishikawa, J.J. Bao, Y. Yamane, K. Akimaru, K. Frindrich, C.D. Wright, M.T. Kuo, Coordinated induction of MRP/GS-X pump and gamma-glutamylcysteine synthetase by heavy metals in human leukemia cells, J. Biol. Chem. 271 (1996) 14981–14988.
[6] M.T. Kuo, J.J. Bao, S.A. Curley, M. Ikeguchi, D.A. Johnston, T. Ishikawa, Frequent coordinated overexpression of the MRP/GS-X pump and gamma-glutamylcysteine synthetase genes in human colorectal cancers, Cancer Res. 56 (1996) 3642–3644.
[7] Y. Yamane, M. Furuichi, R. Song, N.T. Van, R.T. Mulcahy, T. Ishikawa, M.T. Kuo, Expression of multidrug resistance protein/GS-X pump and gamma-glutamylcysteine synthetase genes is regulated by oxidative stress, J. Biol. Chem. 273 (1998) 31075–31085.
[8] K. Itoh, T. Chiba, S. Takahashi, T. Ishii, K. Igarashi, Y. Katoh, T. Oyake, N. Hayashi, K. Satoh, I. Hatayama, M. Yamamoto, Y. Nabeshima, An Nrf2/small Maf heterodimer mediates the induction of phase II detoxifying enzyme genes through antioxidant response elements, Biochem. Biophys. Res. Commun. 236 (1997) 313–322.
[9] J.D. Hayes, M. McMahon, Molecular basis for the contribution of the antioxidant responsive element to cancer chemoprevention, Cancer Lett. 174 (2001) 103–113.
[10] J.D. Hayes, S.A. Chanas, C.J. Henderson, M. McMahon, C. Sun, G.J. Moffat, C.R. Wolf, M. Yamamoto, The Nrf2 transcription factor contributes both to the basal expression of glutathione *S*-transferases in mouse liver and to their induction by the chemopreventive synthetic antioxidants, butylated hydroxyanisole and ethoxyquin, Biochem. Soc. Trans. 28 (2000) 33–41.
[11] T. Ishii, K. Itoh, S. Takahashi, H. Sato, T. Yanagawa, Y. Katoh, S. Bannai, M. Yamamoto, Transcription factor Nrf2 coordinately regulates a group of oxidative stress-inducible genes in macrophages, J. Biol. Chem. 275 (2000) 16023–16029.

[12] A. Enomoto, K. Itoh, E. Nagayoshi, J. Haruta, T. Kimura, T. O'Connor, T. Harada, M. Yamamoto, High sensitivity of Nrf2 knockout mice to acetaminophen hepatotoxicity associated with decreased expression of ARE-regulated drug metabolizing enzymes and antioxidant genes, Toxicol. Sci. 59 (2001) 169–177.
[13] J.Y. Chan, M. Kwong, Impaired expression of glutathione synthetic enzyme genes in mice with targeted deletion of the Nrf2 basic-leucine zipper protein, Biochim. Biophys. Acta 1517 (2000) 19–26.
[14] M. McMahon, K. Itoh, M. Yamamoto, S.A. Chanas, C.J. Henderson, L.I. McLellan, C.R. Wolf, C. Cavin, J.D. Hayes, The Cap'n'Collar basic leucine zipper transcription factor Nrf2 (NF-E2 p45-related factor 2) controls both constitutive and inducible expression of intestinal detoxification and glutathione biosynthetic enzymes, Cancer Res. 61 (2001) 3299–3307.
[15] M. Ramos-Gomez, M.K. Kwak, P.M. Dolan, K. Itoh, M. Yamamoto, P. Talalay, T.W. Kensler, Sensitivity to carcinogenesis is increased and chemoprotective efficacy of enzyme inducers is lost in nrf2 transcription factor-deficient mice, Proc. Natl. Acad. Sci. USA 98 (2001) 3410–3415.
[16] S.A. Chanas, Q. Jiang, M. McMahon, G.K. McWalter, L.I. McLellan, C.R. Elcombe, C.J. Henderson, C.R. Wolf, G.J. Moffat, K. Itoh, M. Yamamoto, J.D. Hayes, Loss of the Nrf2 transcription factor causes a marked reduction in constitutive and inducible expression of the glutathione *S*-transferase Gsta1, Gsta2, Gstm1, Gstm2, Gstm3 and Gstm4 genes in the livers of male and female mice, Biochem. J. 365 (2002) 405–416.
[17] H. Sasaki, H. Sato, K. Kuriyama-Matsumura, K. Sato, K. Maebara, H. Wang, M. Tamba, K. Ktoh, M. Yamamoto, S. Bannai, Electrophile responsible element-mediated induction of the cystine/glutamate exchange transporter gene expression, J. Biol. Chem. 277 (2002) 44765–44771.
[18] H.M. Kauffmann, S. Pfannschmidt, H. Zoller, A. Benz, B. Vorderstemann, J.I. Webster, D. Schrenk, Influence of redox-active compounds and PXR-activators on human MRP1 and MRP2 gene expression, Toxicology 171 (2002) 137–146.
[19] M. Suzuki, H. Suzuki, Y. Sugimoto, Y. Sugiyama, ABCG2 transports sulfated conjugates of steroids and xenobiotics, J. Biol. Chem. 278 (2003) 22644–22649.
[20] H. Motohashi, T. O'Connor, F. Katsuoka, J.E. Engel, M. Yamamoto, Integration and diversity of the regulatory network composed of Maf and CNC families of transcription factors, Gene 294 (2002) 1–12.
[21] E.M. Leslie, R.G. Deeley, S.P. Cole, Toxicological relevance of the multidrug resistance protein 1, MRP1 (ABCC1) and related transporters, Toxicology 167 (2001) 3–23.
[22] P. Borst, R.O. Elferink, Mammalian ABC transporters in health and disease, Annu. Rev. Biochem. 71 (2002) 537–592.
[23] J. Wijnholds, R. Evers, M.R. van Leusden, C.A. Mol, G.J. Zaman, U. Mayer, J.H. Beijnen, M. van der Valk, P. Krimpenfort, P. Borst, Increased sensitivity to anticancer drugs and decreased inflammatory response in mice lacking the multidrug resistance-associated protein, Nat. Med. 3 (1997) 1275–1279.
[24] A. Lorico, G. Rappa, R.A. Finch, D. Yang, R.A. Flavell, A.C. Sartorelli, Disruption of the murine MRP (multidrug resistance protein) gene leads to increased sensitivity to etoposide (VP-16) and increased levels of glutathione, Cancer Res. 57 (1997) 5238–5242.

0026-895X/03/6405-1018–1028$7.00
MOLECULAR PHARMACOLOGY
Copyright © 2003 The American Society for Pharmacology and Experimental Therapeutics
Mol Pharmacol 64:1018–1028, 2003

Vol. 64, No. 5
2634/1100446
Printed in U.S.A.

Expression of the Aflatoxin B_1-8,9-Epoxide-Metabolizing Murine Glutathione *S*-Transferase A3 Subunit Is Regulated by the Nrf2 Transcription Factor through an Antioxidant Response Element

IAN R. JOWSEY, QING JIANG, KEN ITOH, MASAYUKI YAMAMOTO, and JOHN D. HAYES

Biomedical Research Centre, Ninewells Hospital and Medical School, University of Dundee, Dundee, United Kingdom (I.R.J., Q.J., J.D.H.); and Centre for Tsukuba Advanced Research Alliance and Institute of Basic Medical Sciences, University of Tsukuba, Tsukuba, Japan (K.I., M.Y.)

Received May 5, 2003; accepted July 18, 2003

This article is available online at http://molpharm.aspetjournals.org

ABSTRACT

High expression of the aflatoxin B_1 (AFB_1)-8,9-epoxide-conjugating glutathione *S*-transferase A3 (mGSTA3) subunit in mouse liver confers intrinsic resistance to AFB_1 hepatocarcinogenesis. It is not known how the gene encoding this protein is regulated. The murine *mGSTA3* gene has been identified using bioinformatics. It localizes to mouse chromosome 1 (A3-4), spans approximately 24.6 kilobases (kb) of DNA, and comprises seven exons. High levels of mGSTA3 mRNA are present in organs associated with detoxification. Expression of mGSTA3 in Hepa1c1c7 mouse hepatoma cells was found to be inducible by sulforaphane, an organic isothiocyanate that can transcriptionally activate genes through the antioxidant response element (ARE). Sulforaphane also induced transcription of a luciferase reporter containing a 1.5 kb fragment of the *mGSTA3* 5′-upstream region. A putative ARE, with sequence 5′-TGACATTGC-3′, was identified within this fragment, approximately 150 base pairs upstream of exon 1. Mutation of this sequence abrogated both basal and sulforaphane-inducible reporter activity. Overexpression of the basic-region leucine zipper Nrf2 transcription factor augmented activity of the *mGSTA3*-luciferase reporter through this ARE. Electrophoretic mobility shift assays demonstrated that Nrf2 binds the *mGSTA3* ARE. Measurement of mGSTA3 mRNA levels in tissues isolated from both wild-type and *nrf2*-null mice revealed that loss of the Nrf2 transcription factor is associated with a reduction in basal expression of mGSTA3. Collectively, these data demonstrate a role for Nrf2 and the ARE in regulating transcription of *mGSTA3*.

Aflatoxin B_1 (AFB_1), a difuranocoumarin mycotoxin produced by the mold *Aspergillus flavus*, is a potent naturally occurring carcinogen (Eaton and Gallagher, 1994). Its harmful effects arise because of biotransformation to AFB_1-8,9-*exo*-epoxide (Fig. 1), a metabolite that can react readily with the N^7 atom of guanine residues in DNA. Consistent with this observation, AFB_1-initiated liver tumors in the rat often contain G→T and G→A mutations in codon 12 of *ras* oncogenes (McMahon et al., 1990), whereas in human hepatocytes, exposure to AFB_1 produces mutations within the *p53* tumor suppressor gene (Aguilar et al., 1993).

The toxicity of AFB_1 varies significantly between species. Whereas rats are sensitive to AFB_1 hepatocarcinogenesis, many mouse strains can tolerate exposure to the mycotoxin (Eaton and Gallagher, 1994; Hengstler et al., 1999). This selective toxicity reflects a differential ability of mouse and rat to detoxify AFB_1-8,9-epoxide through glutathione (GSH) conjugation. The species differences in hepatic AFB_1-GSH conjugating activity is caused by the constitutive expression in mouse liver of a class α glutathione *S*-transferase subunit (mGSTA3 or Yc) that exhibits high catalytic activity toward the mycotoxin (Buetler et al., 1992; Hayes et al., 1992). Support for this hypothesis was provided by the finding that ectopic expression of mGSTA3 in hamster V79 cells confers resistance to AFB_1 cytotoxicity and causes a reduction in formation of DNA adducts (Fields et al., 1999). A rat class α GST subunit (rGSTA5 or Yc_2) exhibiting significant AFB_1-GSH conjugating activity has also been identified (Hayes et al., 1991, 1994). Although this subunit is constitutively present only at low levels, expression of rGSTA5 is highly

This work was supported by the Association for International Cancer Research (grant 01-096) and the Medical Research Council (grant G0000281).

ABBREVIATIONS: AFB_1, aflatoxin B_1; GSH, glutathione; GST, glutathione *S*-transferase; ARE, antioxidant response element; NQO1, NAD(P)H: quinone oxidoreductase 1; NF-E2, nuclear factor-erythroid 2; bZIP, basic-region leucine zipper; CNC, cap 'n' collar; Nrf, nuclear factor-erythroid 2 p45-related factor; Sul, sulforaphane; MTC, multiple tissue cDNA; PCR, polymerase chain reaction; RACE, rapid amplification of cDNA ends; FISH, fluorescence in situ hybridization; kb, kilobase(s); bp, base pair(s); SSC, standard saline citrate; DAPI, 4,6-diamidino-2-phenylindole; DMSO, dimethyl sulfoxide; EMSA, electrophoretic mobility shift assay; RT-PCR, reverse transcription-polymerase chain reaction.

inducible by a number of cancer chemopreventive agents that provide protection against AFB_1 hepatocarcinogenesis (Hayes et al., 1998; Kelly et al., 2000). Although there is a strong association between either constitutive or induced expression of GST capable of metabolizing AFB_1-8,9-epoxide and resistance to the carcinogenic effects of the mycotoxin, little is known about the mechanisms that regulate the genes encoding these enzymes.

Genes encoding certain detoxification enzymes are transcriptionally regulated through an enhancer known as the antioxidant response element, or ARE (Hayes and McMahon, 2001). This enhancer was first identified as a regulatory element within the rat (*rGSTA2*) 5′-upstream region that conferred transcriptional responsiveness to β-naphthoflavone (Rushmore et al., 1990). Subsequently, the ARE has been shown to mediate a transcriptional response to a broad spectrum of structurally diverse xenobiotics (Nguyen et al., 2003). Mutational analysis of the 5′-upstream region of *rGSTA2* led to the identification of the ARE sequence required for both basal and/or inducible activity as 5′-TGACnnnGC-3′ (Rushmore et al., 1991). Other genes known to be regulated through an ARE include those encoding mouse GSTA1, mouse, human and rat NAD(P)H:quinone oxidoreductase (NQO1), human glutamate cysteine ligase catalytic and regulatory subunits, and mouse heme oxygenase-1 (Nguyen et al., 2003; Nioi et al., 2003).

The identity of the transcription factors that mediate regulation of ARE-driven genes has stimulated much interest. The similarity between the ARE and the binding motif for nuclear factor-erythroid 2 (NF-E2) lead to the supposition that this transcription factor may regulate the expression of ARE-containing genes. NF-E2 is a dimeric protein composed of 45-kDa (p45) and 18-kDa (p18) subunits, each belonging to the basic-region leucine zipper (bZIP) transcription factor superfamily (Motohashi et al., 2002). The restricted expression of the p45 subunit to hematopoietic tissues was not consistent with it being involved in regulating the transcription of hepatic genes. However, the related cap 'n' collar (CNC) bZIP family members, NF-E2 p45-related factors 1 and 2 (Nrf1 and Nrf2) exhibit a more ubiquitous tissue-specific expression profile (McMahon et al., 2001). Numerous studies since have shown that these transcription factors activate target gene expression through the ARE (for review, see Nguyen et al., 2003). Of particular relevance to the selective toxicity of AFB_1 is the observation that expression of mGSTA3 is reduced in mouse lines with targeted disruption of CNC bZIP genes. Specifically, red blood cells from *NF-E2 p45*-nulled mice show a marked reduction in mGSTA3 (Chan et al., 2001). Also, liver and small intestine from $nrf2^{-/-}$ mice express less mGSTA3 than $nrf2^{+/+}$ mice (McMahon et al., 2001; Chanas et al., 2002; Thimmulappa et al., 2002). Although CNC bZIP proteins are clearly involved in regulating the expression of the transferase, it is unclear whether these transcription factors act directly through an ARE present in the *mGSTA3* 5′-upstream sequence. Functional characterization of the *mGSTA3* regulatory region has been undertaken as a first step to establish the molecular genetic basis for the intrinsic resistance of the mouse to AFB_1.

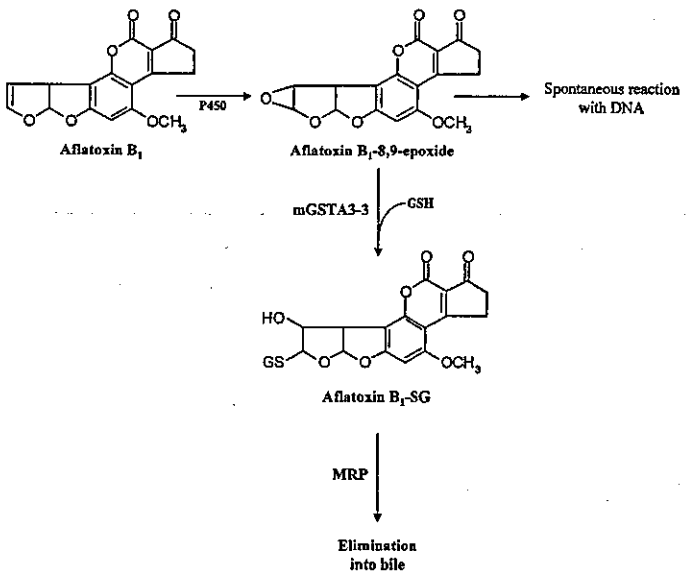

Fig. 1. Metabolism of aflatoxin B_1. The initial 8,9-epoxidation of AFB_1 is catalyzed by cytochrome P450. Mouse GSTA3-3 catalyzes the conjugation of GSH to AFB_1-8,9-epoxide, thus targeting this genotoxic metabolite for elimination from the cell via the multidrug resistance protein (Loe et al., 1997). MRP, multidrug resistance protein.

Materials and Methods

Chemicals and Reagents. Unless stated otherwise, all chemicals were obtained from Sigma Chemical (Poole, Dorset, UK). Sulforaphane (Sul) (>98% pure) was purchased from LKT Laboratories (St. Paul, MN). Oligonucleotide primers were supplied by MWG Biotech (Ebersberg, Germany) and are listed in Table 1. Restriction endonucleases were obtained from Roche Diagnostics Ltd. (Lewes, E. Sussex, UK).

Tissue-Specific Expression of mGSTA3. The tissue-specific expression of *mGSTA3* and mouse *GAPDH* (*mGAPDH*) was examined using a multiple tissue cDNA (MTC) panel (BD Biosciences Clontech, Palo Alto, CA). This panel comprised pooled first-strand cDNA preparations isolated from eight mouse tissues. The panel is supplied after normalization to four different housekeeping genes. The relative abundance of mGSTA3 cDNA in each tissue sample was determined by PCR using the MA3MTC-A/MA3MTC-B primer pair (Table 1). The relative expression of mGAPDH in the tissue samples was examined using primers supplied with the panel. The PCR reaction was carried out in a 50-μl volume, containing reaction buffer (5 μl), 200 μM each of dATP, dCTP, dGTP, and dTTP, 0.4 μM of each primer, 1 ng of cDNA from each tissue, and TITANIUM *Taq*DNA polymerase (1 μl). The template was denatured initially through incubation at 94°C for 30 s; thereafter, amplification was achieved by denaturation at 94°C for 30 s followed by primer annealing/extension at 68°C for 30 s. Agarose-gel electrophoresis was used to examine PCR products after successive rounds of amplification to ensure linearity of the reaction.

Cell Culture. Unless stated otherwise, all cell culture reagents were obtained from Invitrogen (Paisley, Renfrewshire, UK). Mouse hepatoma Hepa1c1c7 cells were supplied by the European Collection of Animal Cell Cultures (Porton Down, Salisbury, UK) and were maintained in minimal essential medium Eagle, α modification (Sigma Chemical) supplemented with 10% (v/v) heat-inactivated fetal bovine serum, 50 units/ml penicillin/streptomycin, and 2 mM L-glutamine. Cells were incubated at 37°C in a humidified atmosphere of 5% CO_2 in air.

SDS-PAGE and Western Blot Analysis. Discontinuous SDS-PAGE was performed using 12% (w/v) polyacrylamide resolving gels. For Western blot analyses, proteins resolved by SDS-PAGE were transferred to Immobilon-P as described previously (Ellis et al., 1996). Membranes were incubated with primary antibodies specific for mGSTA3 (McLellan et al., 1991) or rat lactate dehydrogenase (Ellis et al., 1996). Specific binding of immobilized proteins was

detected with goat anti-(rabbit IgG) secondary antibodies conjugated with horseradish peroxidase (Bio-Rad, Hemel Hempstead, Hertfordshire, UK). Secondary antibody complexes were visualized using enhanced chemiluminescence and autoradiography.

DNA Sequence Analysis. Sequence analysis was carried out by the DNA Sequencing Laboratory (Department of Molecular and Cellular Pathology, Ninewells Hospital, University of Dundee, Scotland, UK).

5′-Rapid Amplification of cDNA Ends (5′-RACE). The 5′ sequence of the mGSTA3 transcript was determined using the SMART RACE cDNA amplification kit (BD Biosciences Clontech, Hampshire, UK) in accordance with the manufacturer's instructions. Total RNA isolated from Hepa1c1c7 cells was used as the template for reverse transcription using the gene-specific primer MA3RACE (Table 1). Reaction products were subcloned into the pCR2.1 vector (Invitrogen) and sequenced from T7 and M13 (reverse) priming sites. The sequence of eight individual clones was determined.

Identification of the *mGSTA3* Gene. The *mGSTA3* gene was identified using the BLAT search facility available through the University of California Santa Cruz (Genome) World Wide Web site (http://www.genome.ucsc.edu). The mGSTA3 mRNA sequence derived from the 5′-RACE experiments and previous studies (Hayes et al., 1992) was used to search against the February 2002 mouse genome data assembly.

Chromosomal Localization of the *mGSTA3* Gene. The chromosomal localization of the *mGSTA3* gene was confirmed by fluorescence in situ hybridization (FISH) analysis of mouse metaphase chromosomes. A 9.7-kb fragment of the *mGSTA3* gene was first amplified as a probe from mouse genomic DNA by long-range PCR using primers MA3CL-A and MA3CL-B. The reaction was performed in a 50-μl volume, containing reaction buffer (5 μl), 200 ng of each primer, 400 μM each of dATP, dCTP, dGTP, and dTTP, 5 units of Herculase DNA polymerase (Stratagene, Amsterdam, The Netherlands), and 1 μg of mouse genomic DNA as template. Amplification was carried out using a ThermoHybaid PCR Sprint temperature cycling system (ThermoHybaid, Ashford, Middlesex, UK). Samples were heated initially to 92°C for 2 min. Preliminary amplification was achieved over 10 cycles comprising denaturation at 92°C for 10 s, primer annealing at 58°C for 30 s, and extension at 68°C for 11 min. This was followed immediately by 20 cycles involving denaturation at 92°C for 10 s, primer annealing at 58°C for 30 s, and extension at 68°C for 11 min 10 s. The reaction was completed with a single incubation at 68°C for 10 min. The reaction product was subcloned into the pBluescript KS⁻ vector (Stratagene). Successful amplification of the desired target was confirmed using a combination of restriction analysis and DNA sequence analysis. FISH analysis was performed by ChromBios GmbH (Raubling, Germany). Probe DNA (1.5 μg) consisting of the 9.7-kb *mGSTA3* genomic fragment in pBluescript KS⁻ was labeled by standard nick translation. Digoxigenin (Roche Diagnostics Ltd.) was used as labeled dUTP at a concentration of 40 μM. An optimal average probe length of approximately 300 bp was confirmed by agarose-gel electrophoresis.

Chromosomes were prepared according to standard cytogenetic techniques (further details available at www.chrombios.com). Excess cytoplasm was removed from slides by treating with pepsin (0.5 mg/ml in 0.01 M HCl, pH 2.0) at 37°C for 30 min and washing at room temperature with phosphate-buffered saline (2 × 10 min) followed by phosphate-buffered saline containing 50 mM $MgCl_2$ (1 × 10 min). Chromosome denaturation was achieved by submerging slides in 2× SSC containing 70% (v/v) formamide for 1 min at 70°C. Thereafter, slides were dehydrated through successive exposure to 70% (v/v), 90% (v/v), or absolute ethanol for 5 min, followed by air drying. Approximately 50 ng of the labeled DNA probe was resuspended in 15 μl of hybridization solution [2× SSC containing 50% (v/v) formamide] and denatured at 75°C for 5 min. The probe was then preannealed at 37°C for 1 h and applied to the denatured chromosomes. The site of hybridization was covered with a 22 × 22-mm coverslip and sealed with rubber cement. Slides were incubated at 37°C for 24 h. The coverslip was removed and the slide washed for 5 min at 45°C in 2× SSC containing 50% (v/v) formamide and then for a further 5 min at 60°C in 0.1× SSC. Signal detection was performed with an anti-digoxigenin antibody labeled with rhodamine (Roche Diagnostics Ltd.) diluted 1:500 in 4× SSC containing 5% (w/v) bovine serum albumin. Slides were incubated in the antibody solution for 30 min and washed twice in 4× SSC containing 0.1% (v/v) Tween for 10 min. Before microscopy, the slides were mounted in antifade solution containing DAPI (Citifluor Ltd., London, UK). Images of metaphase spreads were captured with a cooled charge-coupled device camera (Photometrics Sensys camera equipped with a Kodak KAF1400 chip) coupled to a Zeiss Axioscope 2 microscope (Welwyn Garden City, Hertfordshire, UK). Camera control and digital image acquisition was achieved using SmartCapture software (Digital Scientific, Cambridge, UK). Chromosomes were identified by computer-enhanced DAPI banding. Merging of chromosome images was performed using SmartCapture software.

Isolation of *mGSTA3* 5′-Upstream Sequence. Approximately 1.5 kb of sequence upstream of exon 1 was amplified by PCR from mouse genomic DNA using primers MA3PROM-A and MA3PROM-B (Table 1). Reactions were carried out in a 50-μl volume, containing reaction buffer (5 μl), 1 mM $MgSO_4$, 200 ng of each primer, 400 μM each of dATP, dCTP, dGTP, and dTTP, 500 ng of mouse genomic DNA, and 2.5 units of Platinum *Pfx* DNA polymerase (Invitrogen).

TABLE 1
Oligonucleotide sequences

Oligonucleotide	Sequence (5′ → 3′)
Cloning and PCR-Based Analyses	
MA3MTC-A	CTGGCAAGGTTACGAAGTGATGGGAGTCTG
MA3MTC-B	GTTGCTGACTCTGCTTCTCAGCGCTTTCAG
MA3RACE	CGGGTCCAGCTCTTCCACATGGTAGAGG
MA3CL-A	CTTCAACACCTGAGGAATTCAAGTTG
MA3CL-B	GCAACCAAGAATTCTAGGAATGTCAG
MA3PROM-A	CACATCTCTGCTTCTATTGAGGTG
MA3PROM-B	GCTAGCTTTTACCATATGCAAGAG
MA3MUT1-A	CCAACTCTTTAGCAACTCAGGCAGGCCCTGGAATTTTTCTTCTAATCC
MA3MUT1-B	GGATTAGAAGAAAAATTCCAGGGCCTGCCTGAGTTGCTAAAGAGTTGG
MA3MUT2-A	CCAACTCTTTAGCAACTCAGGCAGGACATTGCATTTTTCTTCTAATCC
MA3MUT2-B	GGATTAGAAGAAAAATGCAATGTCCTGCCTGAGTTGCTAAAGAGTTGG
EMSA Analyses	
A3-WT 1 (top)	GGAAGAAACATATTAACCAACTCTTTAGCAACTCAGGCATGACATTGCATTTTTCTTCTAAT
A3-WT 2 (bottom)	GGATTAGAAGAAAAATGCAATGTCATGCCTGAGTTGCTAAAGAGTTGGTTAATATGTTTCTT
ARE-MUT 1 (top)	GGAAGAAACATATTAACCAACTCTTTAGCAACTCAGGCAGGCCCTGGAATTTTTCTTCTAAT
ARE-MUT 2 (bottom)	GGATTAGAAGAAAAATTCCAGGGCCTGCCTGAGTTGCTAAAGAGTTGGTTAATATGTTTCTT
T-MUT 1 (top)	GGAAGAAACATATTAACCAACTCTTTAGCAACTCAGGCAGGACATTGCATTTTTCTTCTAAT
T-MUT 2 (bottom)	GGATTAGAAGAAAAATGCAATGTCCTGCCTGAGTTGCTAAAGAGTTGGTTAATATGTTTCTT

The amplification reaction was carried out in a ThermoHybaid PCR Sprint temperature cycling system. The template DNA was denatured initially through incubation at 94°C for 2 min. Thereafter, amplification was performed over 30 cycles through denaturation at 94°C for 30 s, primer annealing at 55°C for 2 min, followed by extension at 68°C for 2 min. The reaction was completed with a single incubation at 68°C for 5 min. The reaction product was subcloned into the pCR-Blunt vector (Invitrogen), and the fidelity of the PCR reaction was confirmed by DNA sequence analysis. The *mGSTA3* fragment was excised from this holding vector as a *KpnI/XhoI* fragment and subcloned into the corresponding restriction sites in pGL3-Basic (Promega, Southampton, UK) to give the construct A3-WT.

Site-Directed Mutagenesis. Site-directed mutagenesis was performed using the QuikChange kit (Stratagene), in accordance with the supplier's instructions. The A3-WT construct was used as a template in all reactions. Mutation of alternate nucleotides throughout the core ARE motif, 5′-TGACATTGC-3′, was achieved using primers MA3MUT1-A and MA3MUT1-B to give the construct ARE-MUT. Mutation of the first thymine nucleotide in this core sequence was achieved using primers MA3MUT2-A and MA3MUT2-B to give the construct T-MUT. The entire sequence of the *mGSTA3* promoter region in each construct was confirmed after mutagenesis.

DNA Transfection and Reporter Gene Assays. Cells were transfected at 70% confluence using Lipofectin reagent (Invitrogen), in accordance with the manufacturer's instructions. The pRL-TK *Renilla reniformis* luciferase reporter vector was included in all samples to provide an internal control for transfection efficiency. In some instances, cells were treated 18 h after transfection with either 5 μM Sul or 0.1% (v/v) DMSO. In all experiments, cells were lysed 48 h after transfection and *R. reniformis* and Firefly luciferase activities determined using the Dual-Luciferase reporter assay system (Promega) and a TD-20/20 luminometer (Turner Designs, Inc., Sunnyvale, CA). Firefly luciferase values derived from the *mGSTA3* reporter constructs were normalized to the corresponding *R. reniformis* luciferase activities.

Electrophoretic Mobility Shift Assays (EMSAs). Binding reactions comprising 100 ng each of recombinant mouse Nrf2 and recombinant mouse MafG were incubated at 20°C for 20 min in a buffer containing 20 mM HEPES, pH 7.9, 1 mM EDTA, 50 mM KCl, 5 mM $MgCl_2$, 10% (v/v) glycerol, 1 mM dithiothreitol, and 3 μg of poly(dI:dC). Reactions were supplemented with an internally-labeled double-stranded oligonucleotide probe containing the *mGSTA3* ARE (Table 1) and incubated at 20°C for a further 20 min. For competition experiments, a 25- or 50-fold molar excess of unlabeled double-stranded oligonucleotides containing either the wild-type (A3-WT) or mutant (ARE-MUT and T-MUT) ARE sequences were added to the binding reaction before the addition of the labeled probe. Complexes were resolved at 4°C through a 4.2% (w/v) polyacrylamide gel in 0.5× Tris borate-EDTA and visualized using autoradiography.

TaqMan Semiquantitative RT-PCR. Total RNA was prepared from tissues isolated from either wild-type or *nrf2*$^{-/-}$ mice using RNeasy kits (QIAGEN, Dorking, Surrey, UK). Relative quantification of GSTA3 mRNA transcripts was performed using the PCR-based 5′-nuclease assay with a gene-specific TaqMan oligonucleotide probe, according to methods described previously (Chanas et al., 2002). The TaqMan probe was labeled at the 5′ end with a fluorescent reporter dye (6-carboxyfluorescein), and at the 3′ end with a quencher dye (6-carboxytetramethylrhodamine). Thermal cycling and real-time fluorescence detection were performed on an ABI PRISM 7700 sequence detection system (Applied Biosystems, Foster City, CA). The level of 18S ribosomal RNA was determined as an internal control using reagents purchased from PerkinElmer.

Results

Tissue-Specific Expression of mGSTA3. Insight into gene regulation can be gained by determining whether a given transcription factor is coexpressed with the target gene. Thus, expression of mGSTA3 mRNA was examined in mouse tissues and compared with data documented previously for Nrf2 (McMahon et al., 2001). For these investigations, a panel of normalized cDNA samples isolated from a range of mouse organs was analyzed by semiquantitative PCR (Fig. 2). Reactions specific for either mGSTA3 (i and ii) or mGAPDH (iii) yielded a single amplicon of the predicted size. Consistent with the role of mGSTA3-3 in hepatic detoxification processes, the mRNA encoding this transferase is expressed most abundantly in liver. Relatively high levels of mRNA are also present in lung. After further amplification, robust expression could be detected in kidney and testis. By contrast, mGSTA3 mRNA is represented at relatively low or undetectable levels in heart, spleen, brain, and skeletal muscle. Northern blot analysis of mouse tissue RNA has revealed that the Nrf2 transcript is also expressed abundantly in kidney, liver, and testis, with moderate levels present in heart and spleen. Relatively low levels of Nrf2 mRNA were observed in brain, lung, and skeletal muscle. This compari-

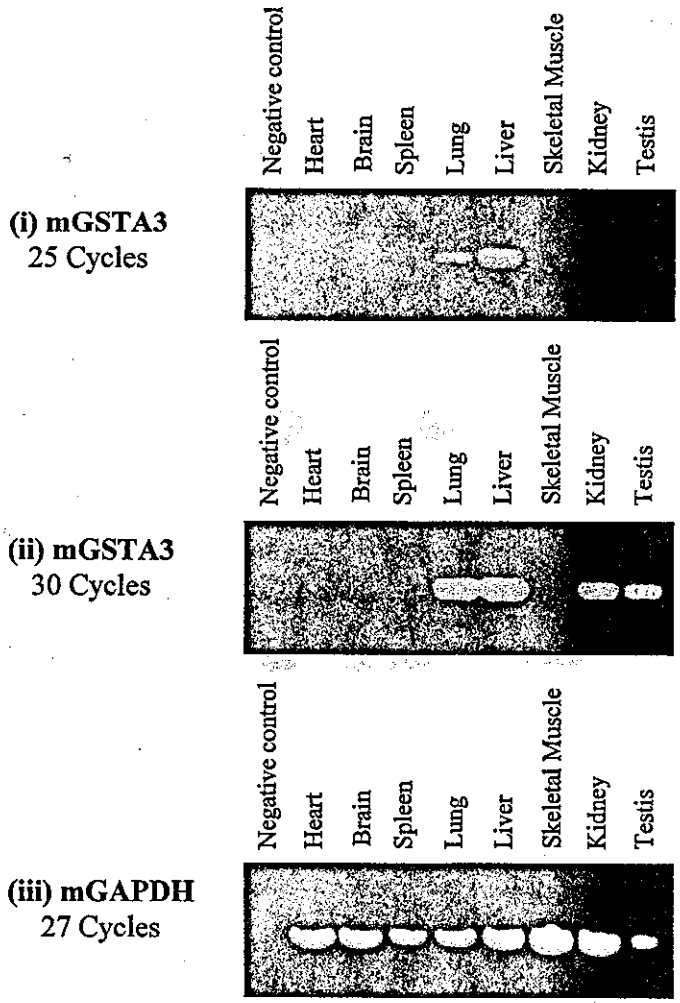

Fig. 2. Tissue-specific expression of mGSTA3 mRNA. A normalized panel of cDNAs isolated from various mouse tissues was analyzed for mGSTA3 (i and ii) and mGAPDH (iii) expression by PCR. Amplification of mGSTA3 was performed over 25 and 30 cycles. The expression of mGAPDH mRNA was examined as a control. Amplification of GAPDH was performed over 27 cycles. Reaction products were analyzed by agarose-gel electrophoresis.

son demonstrates that the Nrf2 transcription factor and mGSTA3 are coexpressed in a number of tissues.

Expression of mGSTA3 Is Induced by Sulforaphane in Mouse Hepatoma Cells. A wide range of structurally diverse compounds can activate gene expression through the ARE (Nguyen et al., 2003). One such compound is Sul, a naturally occurring isothiocyanate generated as a hydrolysis product of glucosinolates from cruciferous vegetables. The effect of Sul on mGSTA3 expression was thus examined in the mouse Hepa1c1c7 hepatoma cell line (Fig. 3). As a positive control, the ability of the isothiocyanate to influence the expression of a validated ARE-regulated gene was confirmed (i). Consistent with previous observations, expression of mouse NQO1 (mNQ1) was potently induced by Sul in the Hepa1c1c7 cell line (Nioi et al., 2003). Significantly, mGSTA3 expression was also found to be inducible by Sul, albeit to a lesser extent (ii). These data demonstrate that mGSTA3 expression is inducible by a compound known to stimulate ARE-driven gene transcription.

Identification of the *mGSTA3* Gene. To establish the mechanism of mGSTA3 induction by Sul, a direct sequence analysis of the gene promoter was required. It was first necessary to determine the organization of the *mGSTA3* gene. The sequence of the mGSTA3 transcript was derived using a combination of 5′-RACE and previously published data (Hayes et al., 1992), and it was used in a bioinformatics analysis of the mouse genome using the University of California Santa Cruz (Genome) worldwide Web site. This analysis revealed that the mGSTA3 transcript is encoded by seven exons, spanning approximately 24.6 kb of genomic DNA (Fig. 4a). The translation initiation and termination codons are located within exons 2 and 7, respectively. As such, exon 1 encodes only 5′-untranslated sequence. These gross aspects of genomic organization are conserved in genes encoding other class α GST (Daniel et al., 1987; Rohrdanz et al., 1992; Rozen et al., 1992; Fotouhi-Ardakani and Batist, 1999). A more detailed comparison was made between the *mGSTA3* gene and the previously described rat *GSTA3* (*rGSTA3*) gene (Fig. 4b). In addition to this conservation in gross aspects of genomic organization between *mGSTA3* and *rGSTA3*, the positions of the predicted splice junctions are also identical between these genes. Analysis of the sequence flanking these splice junctions reveals that each conforms to the gt-ag rule.

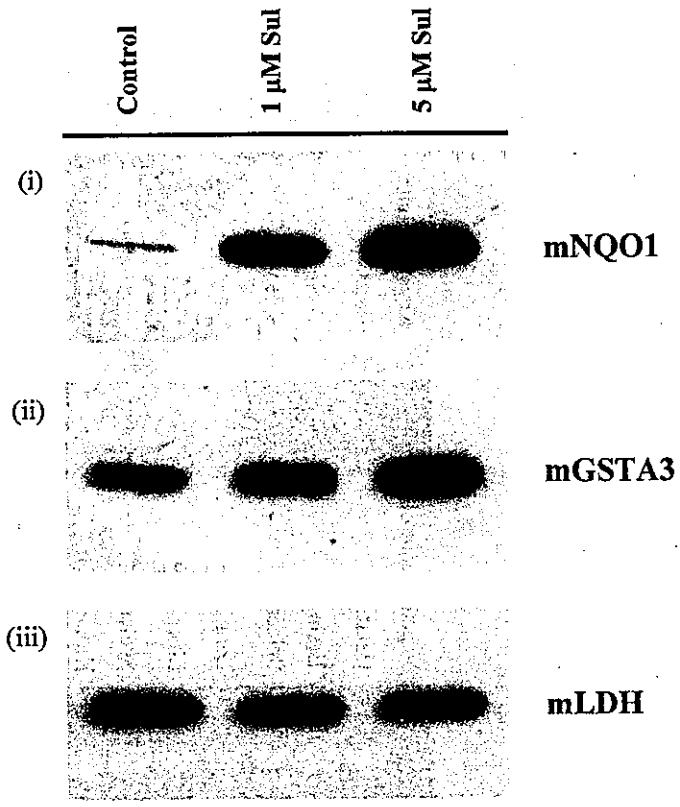

Fig. 3. Effect of sulforaphane on mNQO1 and mGSTA3 expression in Hepa1c1c7 cells. Populations of Hepa1c1c7 cells were treated for 18 h with either Sul (1 μM or 5 μM) or 0.1% (v/v) DMSO (Control). Total cellular protein was isolated and 10 μg of each sample resolved by SDS-PAGE. The expression of mNQO1 (i), mGSTA3 (ii) and mouse lactate dehydrogenase (mLDH) (iii) was examined by Western blot using antibodies described previously (McLellan et al., 1991; Ellis et al., 1996; Kelly et al., 2000).

Chromosomal Localization of *mGSTA3*. The chromosomal localization of murine class α GST has not been examined in great detail. Assembled mouse genome data predicts that the *mGSTA3* gene is located on chromosome 1, region A3-4. Analysis of metaphase mouse chromosomes by FISH confirms this localization (Fig. 5).

Identification of the mGSTA3 5′-Upstream Region. Having determined the organization of the *mGSTA3* gene, the region upstream of exon 1 was next examined (Fig. 6). An A/T-rich TATA box-like sequence was observed approximately 25 nucleotides upstream of exon 1. Other putative promoter elements such as "GC" and "CAAT" boxes were also identified. A detailed search for potential transcription factor binding sites within this 1.5 kb of sequence was performed using the MatInspector version 2.2 software. This sequence-based analysis identified numerous putative regulatory elements. These included a nuclear factor-κB binding site, a glucocorticoid response element, and two barbiturate response elements. The presence of such regulatory elements in other GST genes has been documented (reviewed in Hayes and Pulford, 1995). Of particular relevance in the context of the current study is the presence of a possible ARE located approximately 150 bp upstream of exon 1. The sequence of this putative ARE (5′-TGACATTGC-3′) is identical to the ARE consensus (5′-TGACnnnGC-3′) previously documented by Rushmore et al. (1991). The identification of this ARE-like sequence within the *mGSTA3* 5′-flanking region may provide a molecular basis for the Sul-inducible expression of the transferase observed in Hepa1c1c7 cells.

Identification of a Functional ARE in the *mGSTA3* 5′-Upstream Region. Functional assays were designed to determine whether the *mGSTA3* gene is indeed regulated through an ARE. Approximately 1.5 kb of sequence upstream of exon 1 was amplified by PCR from a mouse genomic DNA template and subcloned into a luciferase reporter vector lacking any native promoter elements (A3-WT). Similar constructs were designed to assess the functionality of the putative ARE (Fig. 7). In the first instance, alternate nucleotides throughout the ARE core were mutated (ARE-MUT). A second construct was created in which only the first nucleotide of the core sequence was substituted (T-MUT). Previous studies have demonstrated that a thymine nucleotide in this position is essential for transcriptional activation through this regulatory element (Rushmore et al., 1991; Nguyen et al., 2000; Nioi et al., 2003). The activity of these

constructs was examined in Hepa1c1c7 cells, in the presence or absence of Sul (Fig. 8). Consistent with the constitutive expression of mGSTA3 in this cell line (Fig. 3), significant activity was detected from the A3-WT vector under basal conditions. Furthermore, mutations within the ARE-like sequence were found to be associated with a dramatic reduction in basal reporter gene activity. Significantly, Sul was found to potentiate transcription of the reporter driven by the wild-type 5′-upstream region of *mGSTA3* around 2-fold. The magnitude of this increase in activity is broadly consistent with the modest induction in mGSTA3 protein expression observed in Hepa1c1c7 cells after treatment with Sul (Fig. 3). By contrast, the isothiocyanate failed to augment the luciferase activity of either the ARE-MUT or T-MUT constructs. The predicted ARE, therefore, mediates the activation of the *mGSTA3* gene by Sul.

Collectively, these data confirm that the *mGSTA3* 5′-upstream region contains a functional ARE that mediates both basal and Sul-inducible transcription in the mouse Hepa1c1c7 cell line.

The *mGSTA3* Gene Is Activated by Nrf2. Having established that the *mGSTA3* gene is regulated through an

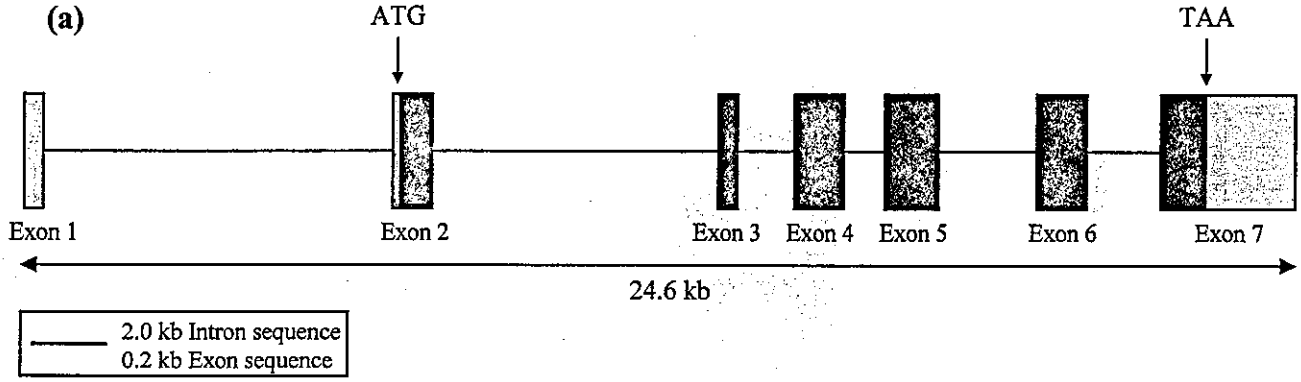

(b)

	EXON 1	**EXON 2**
Mouse *GSTA3*	TAACAAG **gt**aagtactg....Intron 1 (9.1 kb)....ccctgttt**ag**	AAAACCC
Rat *GSTA3*	TAACAAG **gt**aagtactg....Intron 1 (5.0 kb)....ctctgttt**ag**	AGAACTC
	EXON 2	**EXON 3**
Mouse *GSTA3*	TGTGGAG **gt**acgttctg....Intron 2 (7.5 kb)....tgttttct**ag**	TTTGAAG
Rat *GSTA3*	AGTAGAG **gt**aagttctg....Intron 2 (5.1 kb)....tgtttcct**ag**	TTTGAAG
	EXON 3	**EXON 4**
Mouse *GSTA3*	CGAAGTG **gt**aagaaaca....Intron 3 (1.5 kb)....cgtccaat**ag**	ATGGGAG
Rat *GSTA3*	AGGAATG **gt**aagaaaca....Intron 3 (0.9 kb)....catccaat**ag**	ATGGGAG
	EXON 4	**EXON 5**
Mouse *GSTA3*	GAGCCAT **gt**atggtaga....Intron 4 (1.1 kb)....tgtctttc**ag**	CATTGAC
Rat *GSTA3*	GAGCCCT **gt**acggtgac....Intron 4 (1.0 kb)....tgtttttc**ag**	CATCGAC
	EXON 5	**EXON 6**
Mouse *GSTA3*	TGAAAAG **gt**gagtggaa....Intron 5 (2.6 kb)....aattcctc**ag**	GTGTTGA
Rat *GSTA3*	TGAAAAG **gt**gagaggaa....Intron 5 (1.7 kb)....acttcctc**ag**	GTGTTGA
	EXON 6	**EXON 7**
Mouse *GSTA3*	CCTGAAA **gt**actctaca....Intron 6 (1.9 kb)....tctgttgc**ag**	GCGCTGA
Rat *GSTA3*	GCTGAAG **gt**actctgtt....Intron 6 (1.7 kb)....tctgttgc**ag**	GCCCTGA

Fig. 4. Organization of the *mGSTA3* gene. The *mGSTA3* gene was identified using the BLAT search facility available through the University of California Santa Cruz (Genome) Web site. The mGSTA3 mRNA sequence was used as the search template. The gene structure is drawn to scale (a). Exons are represented by boxes, whereas introns are represented by lines. Protein-coding regions of exons are shown in black, whereas noncoding sequence is represented in gray. The sequences flanking each of the exon-intron boundaries in *mGSTA3* and *rGSTA3* have been aligned (b). Sequence located within exons is shown in uppercase, whereas sequence located within introns is shown in lowercase. The gt-ag splice donor-acceptor sites are shown in bold.

ARE present in the 5′-upstream sequence, studies were conducted to determine whether the Nrf2 transcription factor is able to modulate gene expression through this regulatory region. The *mGSTA3* constructs were transfected into Hepa1c1c7 cells in the presence or absence of an expression vector containing the mouse Nrf2 open reading frame (Fig. 9). Consistent with the data presented in Fig. 8, significant activity from the A3-WT construct was detectable under basal conditions. This constitutive transcription was again abrogated upon mutation of the ARE. Significantly, overexpression of Nrf2 resulted in an ~10-fold increase in reporter activity from the A3-WT construct. The ability of Nrf2 to transactivate the *mGSTA3* construct was abolished when mutations were introduced within the core ARE sequence. These data demonstrate that the ARE present in the *mGSTA3* 5′-upstream region can be transactivated by Nrf2.

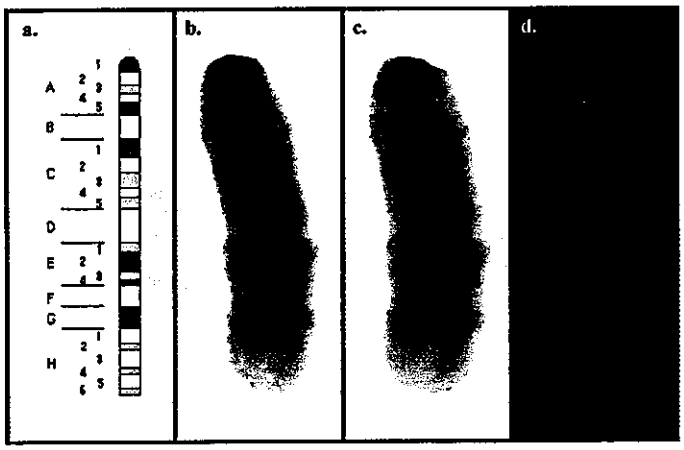

Fig. 5. Chromosomal localization of *mGSTA3*. The chromosomal localization of *mGSTA3* was determined by FISH using a labeled genomic probe. a, idiogram of mouse chromosome 1. b, DAPI-banded chromosome 1. c, DAPI-banded chromosome 1 with the hybridization pattern obtained with the *mGSTA3* probe. d, the same hybridization signal as presented in c showing the original DAPI pattern. More than 40 metaphases were analyzed of which approximately 61% displayed at least one hybridization signal on the four different chromatids, at this region of the chromosome.

Nrf2 Binds the *mGSTA3* ARE. EMSA analyses were performed to determine whether Nrf2 binds the *mGSTA3* ARE (Fig. 10). Because the interaction of Nrf2 with the ARE is dependent upon the formation of a heterodimeric complex with small Maf bZIP proteins (for review, see Motohashi et al., 2002), binding reactions were performed in the presence of both recombinant Nrf2 and recombinant MafG. These analyses demonstrated that a labeled oligonucleotide probe containing the wild-type *mGSTA3* ARE was bound efficiently in the presence of Nrf2/MafG (lanes 1 and 2). Competition EMSA experiments were also performed to determine whether the mutations shown to abolish ARE activity in the ARE-MUT and T-MUT constructs also influenced Nrf2/MafG binding. Although association with Nrf2/MafG could be effectively competed with a 25- or 50-fold molar excess of unlabeled A3-WT *mGSTA3* ARE (lanes 3 and 4), neither the ARE-MUT (lanes 5 and 6) nor T-MUT (lanes 7 and 8) mutant forms of the ARE similarly competed for binding. Thus, Nrf2/MafG does not seem to exhibit significant binding activity for these mutant forms of the ARE.

Expression of *mGSTA3* Is Regulated by Nrf2 in Vivo. The data described above demonstrate that Nrf2 and mGSTA3 are coexpressed in a number of tissues. Further-

```
-1507  CACATCTCTGCTTCTATTGAGGTGCCTGCCACCATATTGAAAGTGTCGTGTGGGTTATTAAAGATGAACTCATATCAAGT
                                                  BRE
-1427  TCCACAAATTAAGAACATCTGTAAAGACCTTTTTCCAAATTCAATTCTATTTACAAGAGCCTAGGATTTGGACATGGGTC

-1347  TAACTTTGAGGGAAGGCACATGATAAACTTAACTCATTCTACAATATAGTTAACAAAAAACTGACAAGTTATCAATCTGA

-1267  GTGATAGAATGTATTTGGGGTTTTTAAAAATACTATTCCTCTTTTGTGTTTTTGGTAGAAATTATTGCAACCATTCTAAA

-1187  TTAATTTGCTGCTACTATCTATGGTCATATTTTTATGCCCATTTATAGGGACTTGACACATACCACAGCCCATGAGAGCA

-1107  CTTGAAACATATAATGTAAAAATAATTCAGGACACAATAATTGAGAAAATGAAATAGTAGCTGATAGTCAGGAGTCTAAC

-1027  TGAACACAGGGCACATGCAAAGGCCTTTTGCGGAGAAGGTAACATCTAGGACAGCCATGTCAATGTGAAGTTCAAAGATA

-947   ACATCTCTTTTTAGCATAAGCACATTCCCTCAATACTTGTGACATACTAATAATCACTACCTGAAACTCAGCTCGTTGTG

-867   GGGTCTGCTTAAATCCAACATAATTCAAACAGCAGGTCAATGCAGTTGACAAAAATTTGATTGTAATCAAGCCACTACTG

-787   CTCAATCAGGGCCACAGATCAGACTTGGGAGCTGAACTAAGACCCTGAAGGGATGCTATCCATCATATTTATAGTATGAA

-707   ACCGTAAAGAGATGGGATGCTAGGGGGGCTATAGCATTGTCTAATCATACTTTGATATAAGGGACTGAGCAAGGAAGTTT

-627   CCATTAATCAAGAGTGGAGTTGATTCCTGAGCCTGGGAAGATGAACTTAGGTTGACCTTGCCAGCAAGTTGGAGAAGTTG
                                                                                  GRE
-547   TCCTTGAGATGTCTGCACTCAGACAGCTGTTTCCTTACAACAGAAGCTGGTCAGCTACTGGGAAGTTCCCAGCTCCCTAG
                                                                  NF-κB
-467   GGCCTGAGACCTTGAATTTAATTTTTTTCTTAGGATTAAATGGAGTCTGAAACCAAACTGGTAGTACCTAGAATGAGGTT

-387   CTATTGCTTGTTCCCAACAAGATTATCTGTTCTGTACCTAACCTGGTGGCCCAGTCCACAGAAGTACTCCCTGGTGTCAC

-307   CAGAGTTCTCTTTATAACATCTGCCAGCTGAGATTTCCCACTTGCTTTAGCCCATCCTCATTGACAGCCGAAGAGTTAAC
                                          BRE
-227   TCTGCTTGGAACAGGTTCTTCCAGCTTGCCATTGGCATTGAGGAAGAAACATATTAACCAACTCTTTAGCAACTCAGGCA

-147   TGACATTGCATTTTTCTTCTAATCCTTTATCTAAATGTCTGGCCTCTGAACACTGTGGGAGTAGCTTTTCCCTTATTGGA
         ARE                                                                      CAAT
-67    TTGTCTCCCCTTAACTGGGAAGGGCGTATTCAAATTTAATAAGTAGCTTACAAAACAGCAGAAACTCT
                                  GC              TATA
```

Fig. 6. Sequence of the *mGSTA3* 5′-upstream region. The 5′-upstream region of *mGSTA3* was identified using assembled mouse genome data available through the University of California Santa Cruz (Genome) worldwide Web site. The sequence of the 5′-flanking region was confirmed by direct DNA sequence analysis after amplification by PCR from mouse genomic DNA. Putative regulatory elements were identified using MatInspector version 2.2 software. The + 1 site was assigned based upon data derived through 5′-RACE showing that the 5′-ends of mGSTA3 transcripts localized around this region and the presence of the putative TATA box approximately 25 bp upstream. A number of potential promoter and regulatory elements are underlined. NF-κB, nuclear factor-κB binding site; GRE, glucocorticoid response element; BRE, barbiturate response element.

more, it is clear that Nrf2 can bind and transactivate the *mGSTA3* gene through the ARE. It was next necessary to determine whether Nrf2 regulates *mGSTA3* gene expression in vivo. The expression of mGSTA3 mRNA was examined in a range of tissues, isolated from groups of either wild-type or Nrf2-null mice (Fig. 11). A sensitive TaqMan quantitative RT-PCR assay was used for this study. Analysis of relative mRNA levels revealed that, in all of the tissues examined, loss of the Nrf2 transcription factor is associated with reduced expression of mGSTA3 mRNA. This effect was most pronounced in small intestine, large intestine and stomach, in which expression levels in *nrf2*$^{-/-}$ mice were less than 6% of the levels observed in wild-type animals. Expression of the transferase in Nrf2-null liver, lung, and kidney was reduced to between 15 and 45% of the level in wild-type tissues.

Discussion

Constitutive expression of mGSTA3 confers intrinsic resistance to the mouse against AFB_1 hepatocarcinogenesis (Fig. 1). Although data derived from null mice have implicated NF-E2 p45 and Nrf2 in the transcriptional regulation of *mGSTA3*, it was previously unclear whether the effects of these CNC bZIP factors were mediated directly through an ARE. The present study demonstrates that the *mGSTA3* 5′-flanking sequence contains a functional ARE. The in vivo role of Nrf2 in regulating *mGSTA3* expression in lung and throughout the gastrointestinal tract (targets of AFB_1 toxicity) has been revealed through analysis of tissue samples derived from either wild-type or *nrf2*$^{-/-}$ mice.

Most class α GST genes in human, rat, and mouse have been shown to comprise seven exons, with the first being a noncoding exon (Daniel et al., 1987; Rohrdanz et al., 1992; Rozen et al., 1992; Fotouhi-Ardakani and Batist, 1999). Together, these observations suggest that the ancestral gene structure of class α GST has been conserved. The present study demonstrates that the *mGSTA3* gene also comprises seven exons. However, at 24.6 kb, *mGSTA3* is relatively large, in that other characterized class α GST genes span between 11 and 15 kb. Interestingly, the *rGSTA5* gene is predicted to comprise only six exons (Pulford and Hayes, 1996). It apparently lacks the first exon equivalent to that encoding the 5′-untranslated sequence in other class α GST genes. The organization of the protein-coding region of the *rGSTA5* gene is, nevertheless, comparable with that of other class α GST genes. It is thus possible that *rGSTA5* does indeed comprise seven exons, but the gene may be under the control of two promoters; one upstream of the as yet unidentified exon 1, whereas the previously identified promoter actually resides within the first intron.

The present study demonstrates that in the Hepa1c1c7 mouse hepatoma cell line, the *mGSTA3* ARE mediates both constitutive and Sul-inducible expression of the transferase. The *mGSTA3* 5′-upstream sequence was found to confer marked luciferase reporter activity under basal conditions in this cell line (Figs. 8 and 9). This observation is consistent with the constitutive expression of the transferase observed in Hepa1c1c7 cells (Fig. 3). This relatively high basal level of mGSTA3 seems to restrict the level of induction that can be achieved after treatment with Sul. Significantly, however, the induction in mGSTA3 expression observed in this study is associated with a comparable increase in reporter activity.

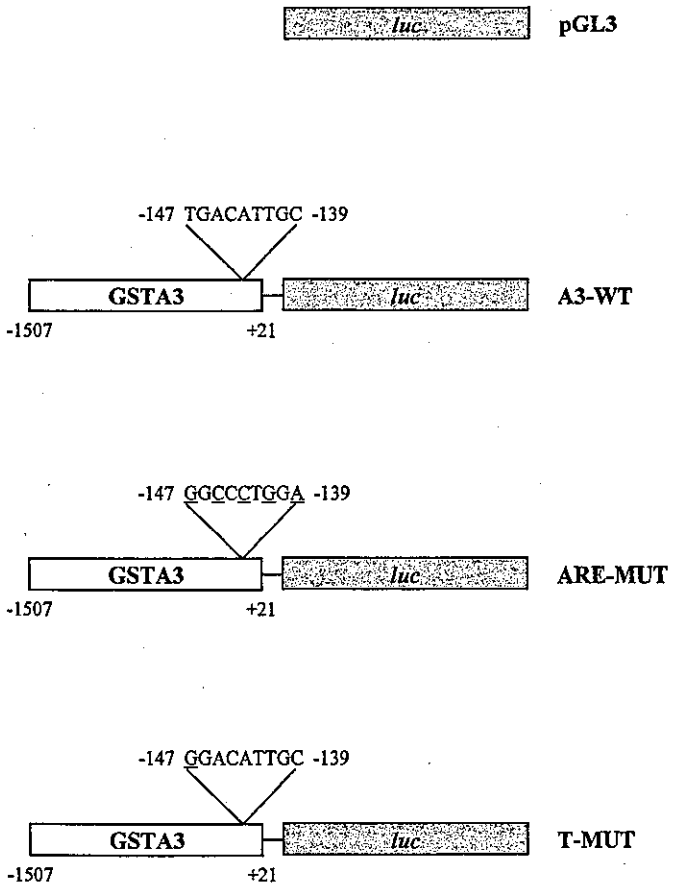

Fig. 7. Design of *mGSTA3* reporter constructs. The functionality of the *mGSTA3* ARE was assessed by generating reporter constructs using the pGL3-Basic luciferase vector (pGL3). Approximately 1.5 kb of sequence from the *mGSTA3* 5′-flanking region was ligated into pGL3-Basic to give the A3-WT construct. A mutant vector (ARE-MUT) was generated in which alternate nucleotides within the ARE core were substituted. A second mutant construct was made in which only the first nucleotide of the core sequence was mutated (T-MUT). The mutations introduced within the ARE core in each construct are underlined.

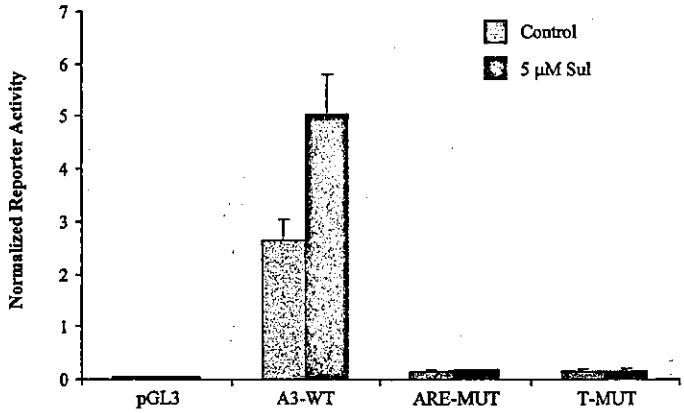

Fig. 8. Effect of sulforaphane on *mGSTA3* reporter activity. Hepa1c1c7 cells were transfected with 600 ng of pGL3, A3-WT, ARE-MUT, or T-MUT *mGSTA3* reporter constructs and 400 ng of pRL-TK *R. reniformis* reporter vector. Approximately 24 h after transfection, cells were treated with either 5 μM Sul or 0.1% (v/v) DMSO (control). Cells were lysed 18 h later and both Firefly (derived from the pGL3-Basic vector) and *R. reniformis* (derived from the pRL-TK vector) luciferase activities determined. All data were normalized to *R. reniformis* internal control luminescence. Results from three independent experiments are expressed as mean normalized reporter activity ± S.D.

In addition to the 5′-TGACATTGC-3′ motif, nucleotides flanking this core enhancer sequence in *mGSTA3* exhibit similarities to AREs found in other genes (Fig. 12). Particularly obvious is the presence of the A/T-rich sequence immediately 3′ of the core "GC" dinucleotide. Despite conservation of the A/T-rich region between AREs in different genes, comprehensive mutational analysis of the *mNQO1* ARE suggests that only the first 5′ "A" is essential for function (Nioi et al., 2003). The region 5′ of the core in *mGSTA3* contains, in reverse orientation, the sequence 5′-TGAGT-3′. A related sequence, 5′-TGACT-3′, is found in a similar position and orientation upstream of AREs in human, rat, and mouse *NQO1* and rat *GSTP1* (*rGSTP1*) and has been shown to be important for both basal and/or inducible expression (Okuda et al., 1990; Favreau and Pickett, 1995; Xie et al., 1995; Nioi et al., 2003). Although there is a single additional nucleotide spacing between this pentanucleotide motif and the ARE core in *mGSTA3* compared with *NQO1* and *rGSTP1*, it is predicted that this flanking sequence in *mGSTA3* is of functional significance. It is unclear which transcription factors bind this upstream 5′-TGAC/GT-3′ sequence, but its similarity to motifs recognized by activator protein-1 and activating transcription factor/cAMP response element-binding protein family members suggests that certain of these proteins may be recruited to the 5′-flanking region of *mGSTA3*, *rGSTP1*, and *NQO1*. In this context, it is noteworthy that Nrf2 can interact with c-Jun and ATF4 (Venugopal and Jaiswal, 1998; He et al., 2001). If the sequence upstream of the core ARE is involved in transcription factor binding, the components of the protein complex recruited to the response element are likely to differ between genes that exhibit heterogeneity in this flanking sequence. In this regard, it is important to recognize that the 5′-TGAC/GT-3′ motif in *mGSTA3*, *rGSTP1*, and *NQO1* is less well conserved in mouse *GSTA1* (*mGSTA1*) and *rGSTA2* (Fig. 12).

In this study, multiple approaches have been used to demonstrate the importance of Nrf2 in regulating mGSTA3 expression through the ARE. First, overexpression of Nrf2 in Hepa1c1c7 cells was found to activate transcription from wild-type, but not mutant, *mGSTA3* reporter constructs. Second, EMSA analyses demonstrated association of the *mGSTA3* ARE with Nrf2/MafG. Furthermore, RT-PCR analyses were adopted to show that mGSTA3 mRNA levels were diminished in tissues isolated from *nrf2*$^{-/-}$ mice, compared with wild-type animals. It is now clear that Nrf1 is also able to stimulate ARE-driven gene expression (Venugopal and Jaiswal, 1996; Hayes and McMahon, 2001; Nguyen et al., 2003). However, the role of this transcription factor in regulating the expression of ARE-dependent genes in vivo has not been established, due to the fact that disruption of *nrf1* in mice confers an embryonically lethal phenotype (Farmer et al., 1997; Chan et al., 1998). Nevertheless, the expression of transcripts encoding GSH-biosynthetic enzymes is reduced in *nrf1*$^{-/-}$ fibroblasts (Kwong et al., 1999). Because certain of these genes are probably regulated through an ARE, these observations are consistent with a role for Nrf1 in regulating ARE-dependent gene expression. Furthermore, loss of NF-E2 p45 is associated with abrogated expression of *mGSTA3* in murine red blood cells (Chan et al., 2001). Figure 11 shows that although loss of Nrf2 is consistently associated with a reduction in mGSTA3 expression levels, the magnitude of this reduction varies between mouse tissues. These observations may reveal the potential for redundancy between CNC bZIP proteins. Thus, although disruption of the *nrf2* gene may have a dramatic impact on the expression of *mGSTA3* in tissues that express little Nrf1, this effect may be diminished in tissues expressing this transcription factor at higher levels.

Although both mouse and rat possess GST capable of metabolizing AFB_1-8,9-epoxide (mGSTA3-3 and rGSTA5-5, respectively), the contrasting sensitivity of these species to AFB_1 hepatocarcinogenesis has been attributed to differences in the constitutive expression levels of these transferases. Whereas robust hepatic expression of mGSTA3 affords the mouse inherent resistance to the mycotoxin, marked induction of the rGSTA5 subunit is necessary to confer protection to the rat. These observations suggest that although mGSTA3 and rGSTA5 are closely related in terms of primary structure and catalytic properties, the genes encoding these transferases are regulated differently in mouse

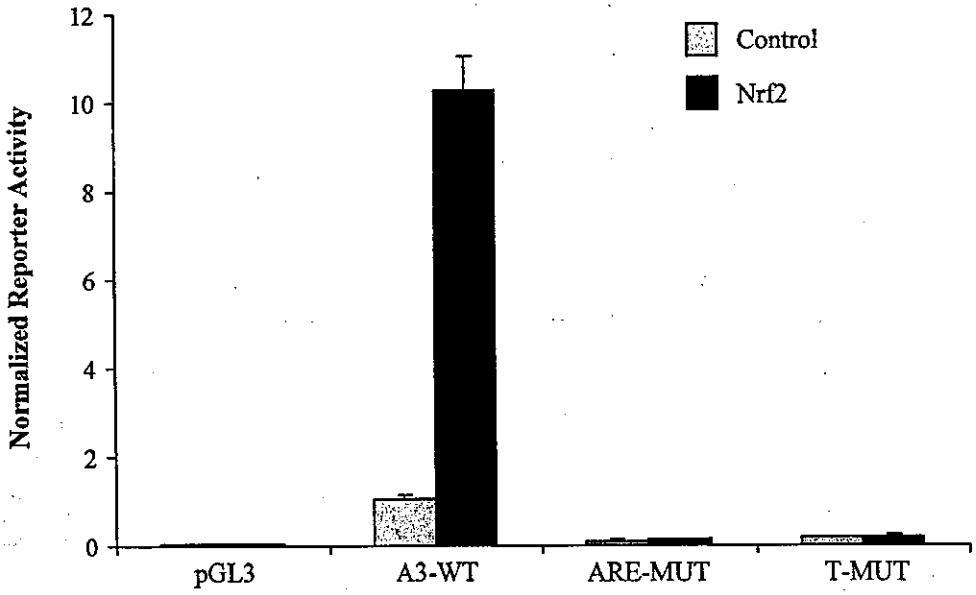

Fig. 9. Effect of Nrf2 overexpression on *mGSTA3* reporter activity. An expression vector encoding V5 epitope-tagged mNrf2 has been described previously (McMahon et al., 2003). Hepa1c1c7 cells were transfected with either 600 ng mNrf2 expression construct (Nrf2) or empty pCDNA3.1 vector (control), 200 ng of either pGL3, A3-WT, ARE-MUT, or T-MUT, and 200 ng of pRL-TK. Cells were lysed 48 h after transfection and both Firefly (derived from the pGL3-Basic vector) and *R. reniformis* (derived from the pRL-TK vector) luciferase activities determined. All data were normalized to *R. reniformis* internal control luminescence. Results from three independent experiments are expressed as mean normalized reporter activity ± S.D.

and rat. This may reflect the presence of distinct regulatory elements in the respective 5′-flanking sequences, or a differing ability to drive basal gene expression through similar regulatory elements. The latter could result from quantitative variations in the availability of transcription factors and/or coactivator proteins, or divergent affinities of conserved regulatory elements for their associated transcription factors. As such, further analysis of the *rGSTA5* gene promoter(s) is required to determine the evolutionary relationship between these transferases and elucidate the molecular basis for their divergent expression levels under basal conditions.

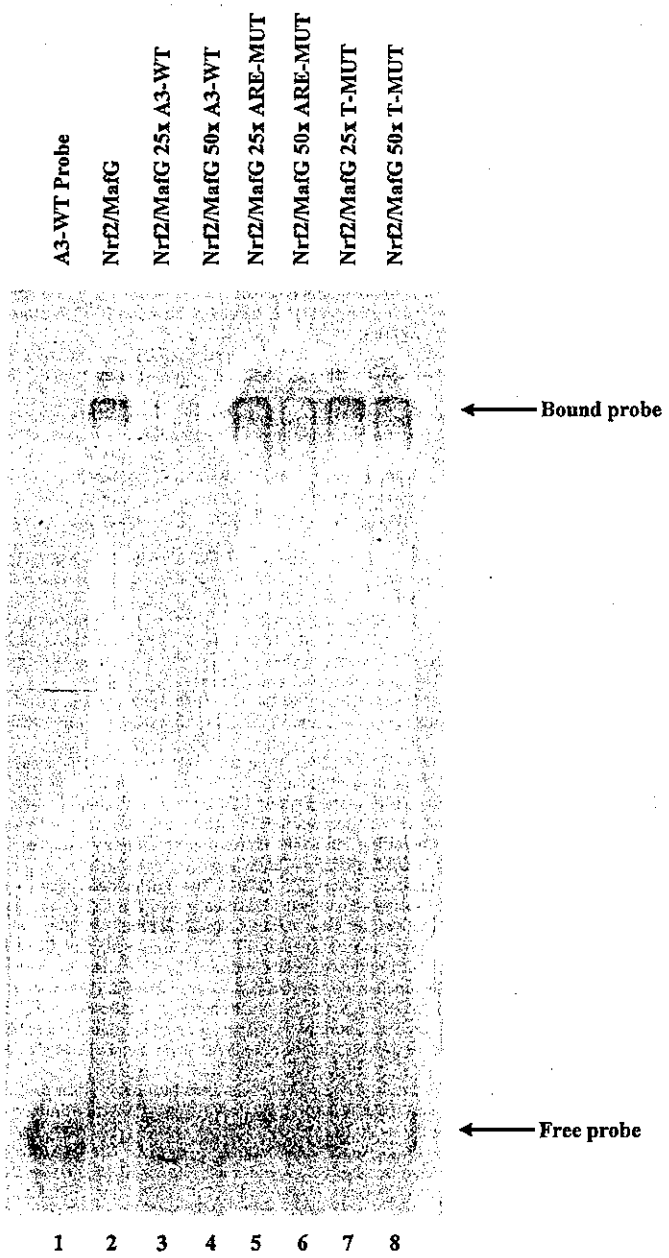

Fig. 10. Association of Nrf2/MafG with the *mGSTA3* ARE. EMSA analyses were performed using recombinant Nrf2 and recombinant MafG in the presence of a radiolabeled double-stranded oligonucleotide probe containing the A3-WT *mGSTA3* ARE (the sequences of the oligonucleotides used in these analyses are presented in Table 1). For competition experiments, reactions were supplemented with a 25- or 50-fold molar excess of competitor DNA. This comprised annealed oligonucleotides containing either the A3-WT ARE, or the mutant sequences shown to abolish enhancer function in the ARE-MUT and T-MUT constructs. Complexes were resolved through a 4.2% (w/v) polyacrylamide gel, run under nondenaturing conditions, and visualized by autoradiography. The positions of bound probe and free probe are indicated by horizontal arrows.

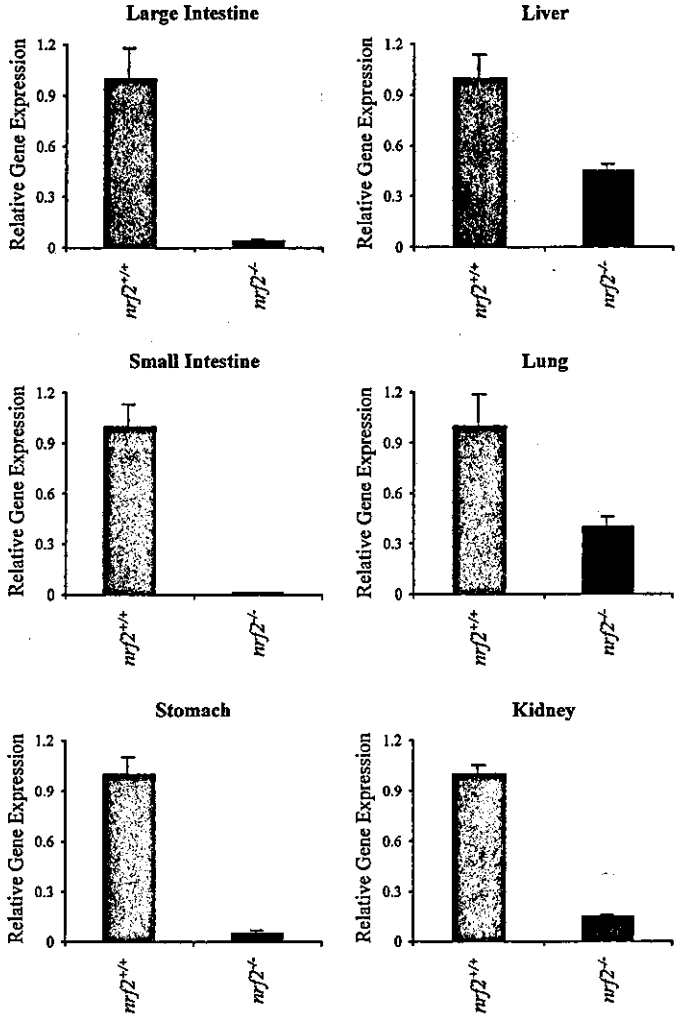

Fig. 11. Nrf2 regulates mGSTA3 expression in vivo. Total RNA was prepared from various tissues isolated from groups (n = 3) of male $nrf2^{+/+}$ or $nrf2^{-/-}$ mice and pooled. Expression of mGSTA3 mRNA was determined in each tissue sample by TaqMan RT-PCR using 18S RNA as an internal control. Assays were performed in triplicate. For each tissue, the expression of mGSTA3 mRNA in Nrf2-null samples is expressed relative to the corresponding wild-type values (set at 1). Values are expressed as means ± S.D.

		'Core' ARE	
mGSTA3	ACTCAGGCA	TGACATTGC	ATTTT
hNQO1	AGTCAC-AG	TGACTCAGC	AGAAT
rNQO1	AGTCAC-AG	TGACTTGGC	AAAAT
mNQO1	AGTCAC-AG	TGAGTCGGC	AAAAT
rGSTP1	AGTCAC-TA	TGATTCAGC	AACAA
mGSTA1	GCTAAT-GG	TGACAAAGC	AACTT
rGSTA2	GCTAAT-GG	TGACAAAGC	AAACT

Fig. 12. Comparison of ARE enhancers. The sequences of various ARE enhancers have been aligned. Data for *hNQO1*, *rNQO1*, *mNQO1*, *rGSTP1*, *mGSTA1*, and *rGSTA2* were taken from Xie et al. (1995), Favreau and Pickett (1995), Nioi et al. (2003), Okuda et al. (1990), Daniel et al. (1987), and Rushmore et al. (1991).

Acknowledgments

We thank Dr. Kerstin Gross-Steinmeyer for helpful discussions about genomic sequence data. We also thank Dr. Clifford R. Elcombe for help in obtaining the TaqMan equipment. It is a pleasure also to acknowledge Michael Mitchell for expert assistance with the bioinformatics analysis.

References

Aguilar F, Hussain SP, and Cerutti P (1993) Aflatoxin B_1 induces the transversion of G→T in codon 249 of the p53 tumor suppressor gene in human hepatocytes. *Proc Natl Acad Sci USA* **90**:8586–8590.

Buetler TM, Slone D, and Eaton DL (1992) Comparison of the aflatoxin B_1-8,9-epoxide conjugating activities of two bacterially expressed alpha class glutathione *S*-transferase isozymes from mouse and rat. *Biochem Biophys Res Commun* **188**: 597–603.

Chan JY, Kwong M, Lo M, Emerson R, and Kuypers FA (2001) Reduced oxidative-stress response in red blood cells from p45 NFE2-deficient mice. *Blood* **97**:2151–2158.

Chan JY, Kwong M, Lu R, Chang J, Wang B, Yen TS, and Kan YW (1998) Targeted disruption of the ubiquitous CNC-bZIP transcription factor, Nrf-1, results in anemia and embryonic lethality in mice. *EMBO (Eur Mol Biol Organ) J* **17**:1779–1787.

Chanas SA, Jiang Q, McMahon M, McWalter GK, McLellan LI, Elcombe CR, Henderson CJ, Wolf CR, Moffat GJ, Itoh K, et al. (2002) Loss of the Nrf2 transcription factor causes a marked reduction in constitutive and inducible expression of the glutathione *S*-transferase Gsta1, Gsta2, Gstm1, Gstm2, Gstm3 and Gstm4 genes in the livers of male and female mice. *Biochem J* **365**:405–416.

Daniel V, Sharon R, Tichauer Y, and Sarid S (1987) Mouse glutathione *S*-transferase Ya subunit: gene structure and sequence. *DNA* **6**:317–324.

Eaton DL and Gallagher EP (1994) Mechanisms of aflatoxin carcinogenesis. *Annu Rev Pharmacol Toxicol* **34**:135–172.

Ellis EM, Judah DJ, Neal GE, O'Connor T, and Hayes JD (1996) Regulation of carbonyl-reducing enzymes in rat liver by chemoprotectors. *Cancer Res* **56**:2758–2766.

Farmer SC, Sun CW, Winnier GE, Hogan BL, and Townes TM (1997) The bZIP transcription factor LCR-F1 is essential for mesoderm formation in mouse development. *Genes Dev* **11**:786–798.

Favreau LV and Pickett CB (1995) The rat quinone reductase antioxidant response element. Identification of the nucleotide sequence required for basal and inducible activity and detection of antioxidant response element-binding proteins in hepatoma and non-hepatoma cell lines. *J Biol Chem* **270**:24468–24474.

Fields WR, Morrow CS, Doehmer J, and Townsend AJ (1999) Expression of stably transfected murine glutathione *S*-transferase A3–3 protects against nucleic acid alkylation and cytotoxicity by aflatoxin B_1 in hamster V79 cells expressing rat cytochrome P450–2B1. *Carcinogenesis* **20**:1121–1125.

Fotouhi-Ardakani N and Batist G (1999) Genomic cloning and characterization of the rat glutathione *S*-transferase-A3-subunit gene. *Biochem J* **339**:685–693.

Hayes JD, Judah DJ, McLellan LI, Kerr LA, Peacock SD, and Neal GE (1991) Ethoxyquin-induced resistance to aflatoxin B_1 in the rat is associated with the expression of a novel alpha-class glutathione *S*-transferase subunit, Yc_2, which possesses high catalytic activity for aflatoxin B_1-8,9-epoxide. *Biochem J* **279**:385–398.

Hayes JD, Judah DJ, Neal GE, and Nguyen T (1992) Molecular cloning and heterologous expression of a cDNA encoding a mouse glutathione *S*-transferase Yc subunit possessing high catalytic activity for aflatoxin B_1-8,9-epoxide. *Biochem J* **285**:173–180.

Hayes JD, Nguyen T, Judah DJ, Petersson DG, and Neal GE (1994) Cloning of cDNAs from fetal rat liver encoding glutathione *S*-transferase Yc polypeptides. The Yc_2 subunit is expressed in adult rat liver resistant to the hepatocarcinogen aflatoxin B_1. *J Biol Chem* **269**:20707–20717.

Hayes JD and Pulford DJ (1995) The glutathione *S*-transferase supergene family: regulation of GST and the contribution of the isoenzymes to cancer chemoprotection and drug resistance. *Crit Rev Biochem Mol Biol* **30**:445–600.

Hayes JD, Pulford DJ, Ellis EM, McLeod R, James RF, Seidegard J, Mosialou E, Jernstrom B, and Neal GE (1998) Regulation of rat glutathione *S*-transferase A5 by cancer chemopreventive agents: mechanisms of inducible resistance to aflatoxin B_1. *Chem Biol Interact* **111–112**:51–67.

Hayes JD and McMahon M (2001) Molecular basis for the contribution of the antioxidant responsive element to cancer chemoprevention. *Cancer Lett* **174**:103–113.

He CH, Gong P, Hu B, Stewart D, Choi ME, Choi AM, and Alam J (2001) Identification of activating transcription factor 4 (ATF4) as an Nrf2-interacting protein. Implication for heme oxygenase-1 gene regulation. *J Biol Chem* **276**:20858–20865.

Hengstler JG, Van der Burg B, Steinberg P, and Oesch F (1999) Interspecies differences in cancer susceptibility and toxicity. *Drug Metab Rev* **31**:917–970.

Kelly VP, Ellis EM, Manson MM, Chanas SA, Moffat GJ, McLeod R, Judah DJ, Neal GE, and Hayes JD (2000) Chemoprevention of aflatoxin B_1 hepatocarcinogenesis by coumarin, a natural benzopyrone that is a potent inducer of aflatoxin B_1-aldehyde reductase, the glutathione *S*-transferase A5 and P1 subunits and NAD(P)H:quinone oxidoreductase in rat liver. *Cancer Res* **60**:957–969.

Kwong M, Kan YW, and Chan JY (1999) The CNC basic leucine zipper factor, Nrf1, is essential for cell survival in response to oxidative stress-inducing agents. Role for Nrf1 in gamma-gcs(l) and gss expression in mouse fibroblasts. *J Biol Chem* **274**:37491–37498.

Loe DW, Stewart RK, Massey TE, Deeley RG, and Cole SP (1997) ATP-dependent transport of aflatoxin B1 and its glutathione conjugates by the product of the multidrug resistance protein (MRP) gene. *Mol Pharmacol* **51**:1034–1041.

McLellan LI, Kerr LA, Cronshaw AD, and Hayes JD (1991) Regulation of mouse glutathione *S*-transferases by chemoprotectors. Molecular evidence for the existence of three distinct alpha-class glutathione *S*-transferase subunits, Ya_1, Ya_2 and Ya_3, in mouse liver. *Biochem J* **276**:461–469.

McMahon G, Davis EF, Huber LJ, Kim Y, and Wogan GN (1990) Characterization of c-Ki-ras and N-ras oncogenes in aflatoxin B_1-induced rat liver tumors. *Proc Natl Acad Sci USA* **87**:1104–1108.

McMahon M, Itoh K, Yamamoto M, Chanas SA, Henderson CJ, McLellan LI, Wolf CR, Cavin C, and Hayes JD (2001) The cap'n'collar basic leucine zipper transcription factor Nrf2 (NF-E2 p45-related factor 2) controls both constitutive and inducible expression of intestinal detoxification and glutathione biosynthetic enzymes. *Cancer Res* **61**:3299–3307.

McMahon M, Itoh K, Yamamoto M, and Hayes JD (2003) Keap1-dependent proteasomal degradation of transcription factor Nrf2 contributes to the negative regulation of antioxidant response element-driven gene expression. *J Biol Chem* **278**: 21592–21600.

Motohashi H, O'Connor T, Katsuoka F, Engel JD, and Yamamoto M (2002) Integration and diversity of the regulatory network composed of Maf and CNC families of transcription factors. *Gene* **294**:1–12.

Nguyen T, Huang HC, and Pickett CB (2000) Transcriptional regulation of the antioxidant response element. Activation by Nrf2 and repression by MafK. *J Biol Chem* **275**:15466–15473.

Nguyen T, Sherratt PJ, and Pickett CB (2003) Regulatory mechanisms controlling gene expression mediated by the antioxidant response element. *Annu Rev Pharmacol Toxicol* **43**:233–260.

Nioi P, McMahon M, Itoh K, Yamamoto M, and Hayes JD (2003) Identification of a novel Nrf2-regulated antioxidant response element in the mouse NAD(P)H: quinone oxidoreductase 1 gene; reassessment of the ARE consensus sequence. *Biochem J* **374**:337–348.

Okuda A, Imagawa M, Sakai M, and Muramatsu M (1990) Functional cooperativity between two TPA responsive elements in undifferentiated F9 embryonic stem cells. *EMBO (Eur Mol Biol Organ) J* **9**:1131–1135.

Pulford DJ and Hayes JD (1996) Characterization of the rat glutathione *S*-transferase Yc_2 subunit gene, GSTA5: identification of a putative antioxidant-responsive element in the 5′-flanking region of rat GSTA5 that may mediate chemoprotection against aflatoxin B_1. *Biochem J* **318**:75–84.

Rohrdanz E, Nguyen T, and Pickett CB (1992) Isolation and characterization of the human glutathione *S*-transferase A2 subunit gene. *Arch Biochem Biophys* **298**: 747–752.

Rozen F, Nguyen T, and Pickett CB (1992) Isolation and characterization of a human glutathione *S*-transferase Ha1 subunit gene. *Arch Biochem Biophys* **292**:589–593.

Rushmore TH, King RG, Paulson KE, and Pickett CB (1990) Regulation of glutathione *S*-transferase Ya subunit gene expression: identification of a unique xenobiotic-responsive element controlling inducible expression by planar aromatic compounds. *Proc Natl Acad Sci USA* **87**:3826–3830.

Rushmore TH, Morton MR, and Pickett CB (1991) The antioxidant responsive element. Activation by oxidative stress and identification of the DNA consensus sequence required for functional activity. *J Biol Chem* **266**:11632–11639.

Thimmulappa RK, Mai KH, Srisuma S, Kensler TW, Yamamoto M, and Biswal S (2002) Identification of Nrf2-regulated genes induced by the chemopreventive agent sulforaphane by oligonucleotide microarray. *Cancer Res* **62**:5196–5203.

Venugopal R and Jaiswal AK (1996) Nrf1 and Nrf2 positively and c-Fos and Fra1 negatively regulate the human antioxidant response element-mediated expression of NAD(P)H:quinone oxidoreductase1 gene. *Proc Natl Acad Sci USA* **93**:14960–14965.

Venugopal R and Jaiswal AK (1998) Nrf2 and Nrf1 in association with Jun proteins regulate antioxidant response element-mediated expression and coordinated induction of genes encoding detoxifying enzymes. *Oncogene* **17**:3145–3156.

Xie T, Belinsky M, Xu Y, and Jaiswal AK (1995) ARE- and TRE-mediated regulation of gene expression. Response to xenobiotics and antioxidants. *J Biol Chem* **270**: 6894–6900.

Address correspondence to: Dr. Ian R. Jowsey, Biomedical Research Centre, Ninewells Hospital and Medical School, University of Dundee, Dundee DD1 9SY, Scotland, UK. E-mail: i.r.jowsey@dundee.ac.uk

MOLECULAR AND CELLULAR BIOLOGY, Dec. 2003, p. 8786–8794 Vol. 23, No. 23
0270-7306/03/$08.00+0 DOI: 10.1128/MCB.23.23.8786–8794.2003

Antioxidants Enhance Mammalian Proteasome Expression through the Keap1-Nrf2 Signaling Pathway

Mi-Kyoung Kwak,[1] Nobunao Wakabayashi,[1,2] Jennifer L. Greenlaw,[1] Masayuki Yamamoto,[2] and Thomas W. Kensler[1]*

Department of Environmental Health Sciences, Johns Hopkins University Bloomberg School of Public Health, Baltimore, Maryland 21205,[1] and Institute of Basic Medical Sciences and Center for Tsukuba Advanced Research Alliance, University of Tsukuba, Tennoudai, Tsukuba 305-8577, Japan[2]

Received 20 June 2003/Returned for modification 6 August 2003/Accepted 26 August 2003

Proteasomes degrade damaged proteins formed during oxidative stress, thereby promoting cell survival. Neurodegenerative and other age-related disorders are associated with reduced proteasome activity. We show herein that expression of most subunits of 20S and 19S proteasomes, which collectively assemble the 26S proteasome, was enhanced up to threefold in livers of mice following treatment with dithiolethiones, which act as indirect antioxidants. Subunit protein levels and proteasome activity were coordinately increased. No induction was seen in mice where the transcription factor Nrf2 was disrupted. Promoter activity of the PSMB5 subunit of the 20S proteasome increased with either Nrf2 overexpression or treatment with antioxidants in mouse embryonic fibroblasts. Tandem antioxidant response elements in the proximal promoter of *PSMB5* that controlled these responses were identified. We propose that induction of the 26S proteasome through the Nrf2 pathway represents an important indirect action of these antioxidants that can contribute to their protective effects against chronic diseases.

Accumulation of abnormal proteins in cells impedes cellular function and can lead cells to apoptosis (6, 39). 26S proteasomes are responsible for the degradation of damaged or misfolded proteins and control levels of key regulatory molecules (6, 15). The proteasome is a large multisubunit complex that contains a proteolytic active 20S core complex consisting of a cylindrical stack of four rings (15). Two inner rings formed with seven β-subunits have proteolytic activity while two outer rings of α-subunits maintain structure. Access to the inner facet of the cylinder is controlled through gating by a 19S regulatory subunit attached to one or both ends. The 19S proteasome participates in the recognition and processing of substrates before their translocation and degradation by the catalytic core (Fig. 1A). The 20S proteasome can directly degrade oxidized proteins, while ubiquitination marks many proteins for recognition and turnover by the entire 26S complex (6). Inhibition of proteasome function induces apoptosis in cancer cells and represents a promising molecular target for oncolytic drugs (1). However, a decreased capacity for protein degradation is related to several neurodegenerative diseases, such as Parkinson's disease, Alzheimer's disease, and amyotrophic lateral sclerosis, in which accumulation of abnormal polypeptides within cells leads to death of neurons, as well as diabetes and atherosclerosis. An altered ubiquitin-proteasome system and reduced proteasome activity are associated with some of these diseases (8, 17, 22, 34). Antioxidants can neutralize oxidative challenges directly by intercepting free radicals (e.g., vitamins C and E) or indirectly by modulating the expression of genes that detoxify these reactive intermediates or eliminate their damage products (9, 10). Sulforaphane and 3*H*-1,2-dithiole-3-thione (D3T), both of which are isolated from cruciferous vegetables (23, 49), as well as the food antioxidant ethoxyquin, activate transcription of protective genes through the antioxidant response element (ARE). The ARE (5′-TGA[C/T]NNN GC-3′) is a *cis*-acting element governing the regulation of multiple phase 2 genes encoding proteins that protect against oxidative and electrophilic stresses, such as glutathione *S*-transferases, γ-glutamylcysteine ligases, and NADPH quinone oxidoreductase (NQO1) (46). The transcription factors that activate the ARE have been extensively studied; the CNC-bZIP ("cap'n'collar" family of basic leucine zipper) protein Nrf2 is an essential element in the transcription complex of the ARE. Studies using *nrf2*-disrupted mice have clearly demonstrated that Nrf2 is a critical factor in the regulation of many cytoprotective genes (19, 25, 43). Induction of these genes by sulforaphane and D3T is largely attenuated in *nrf2*-disrupted mice (25, 43). Moreover, these antioxidants, which are under development as cancer-preventive agents in humans (24, 38), lose their protective efficacy in the *nrf2* knockout mice (11, 35). Because of their altered transcriptional programming, *nrf2*-disrupted mice are considerably more sensitive to the acute and chronic toxicities of environmental chemicals and hyperoxia (2–4, 35). Nrf2 itself is regulated by Keap1, an actin-binding protein that sequesters Nrf2 in the cytoplasm by specific binding to its amino-terminal regulatory domain (20). Indirect antioxidants cause the dissociation of Nrf2 from Keap1, allowing for nuclear accumulation of Nrf2 and enhanced expression of cytoprotective genes. Additional studies of cell systems and *keap1*-disrupted mice demonstrate that the Keap1-Nrf2 complex is a key sensor regulating expression of genes promoting cell survival (44a).

A microarray-based survey of D3T-inducible genes indicated

* Corresponding author. Mailing address: Department of Environmental Health Sciences, Johns Hopkins University Bloomberg School of Public Health, 615 N. Wolfe St., Baltimore, MD 21205. Phone: (410) 955-4712. Fax: (410) 955-0116. E-mail: tkensler@jhsph.edu.

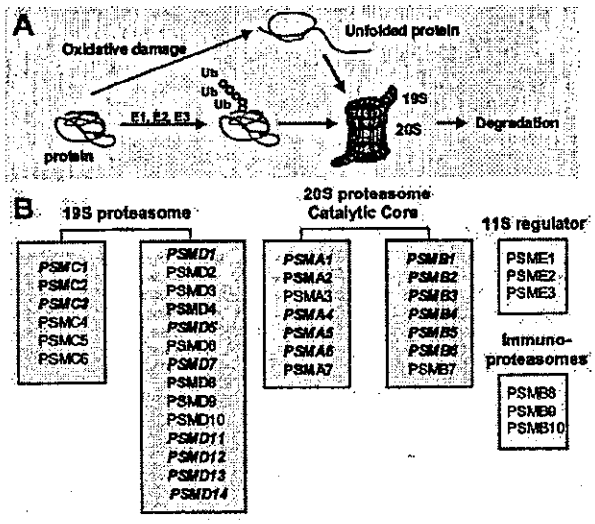

FIG. 1. Microarray summary of proteasome subunits induced in mouse liver by D3T. (A) Proteasomes degrade oxidatively damaged proteins as well as ubiquitin-marked proteins. (B) Subunit components of the 19S and 20S proteasomes. Subunits in boldface italics are genes elevated by D3T in livers of wild-type, but not *nrf2*-disrupted, mice. Subunits in boldface only are genes induced by D3T in both genotypes.

that several hundred genes potentially involved in protection against electrophiles and oxidants were coordinately upregulated (27). Among these genes, multiple proteasome subunits were induced (Fig. 1B). Here we demonstrate that indirect antioxidants, including D3T, increase expression of multiple proteasome subunits through the Keap1-Nrf2-ARE signaling pathway and enhance the activity of the 26S proteasome. Our results indicate that the proteasome genes are prominent downstream targets of the Nrf2 pathway that promotes cell survival.

MATERIALS AND METHODS

Animals and treatment. Wild-type and *nrf2*-disrupted mice were generated from inbred *nrf2* heterozygous mice (25). Mice (10 to 12 weeks old) were fed AIN-76A semipurified diet and treated with D3T (0.5 mmol/kg of body weight) by gavage in a suspension consisting of 1% Cremophor and 25% glycerol. Mice were sacrificed 24 h after treatment, and livers were harvested and snap-frozen. Animal protocols were approved by the Johns Hopkins Animal Care and Use Committee.

Reverse transcription-PCR (RT-PCR) analysis. For the synthesis of cDNAs, 50 ng of total RNA was incubated for 20 min with a solution containing 10 mM Tris (pH 8.4), 5 mM KCl, 5 mM $MgCl_2$, 4 mM deoxynucleoside triphosphates, 0.125 μg of oligo$(dT)_{12-18}$, and 30 U of Moloney murine leukemia virus reverse transcriptase (Life Technologies, Grand Island, N.Y.). PCR amplification for each gene was performed with a Fail Safe PCR kit (Epicentre, Madison, Wis.) using a DNA thermal cycler (MJ Research, Watertown, Mass.). Amplification conditions were 26 or 27 cycles of 5 min at 95°C, 30 s at 56°C, and 40 s at 72°C. Primers were synthesized by Integrated DNA Technology (Coralville, Iowa) and were as follows: *PSMA1*, 5′-TGTTTGACAGACCACTTCCT-3′ and 5′-TCTTCAAGACCATCCAGGAA-3′; *PSMA4*, 5′-TGATGCTAACGTTCTGAC-3′ and 5′-TTCAACATTGACACAGCC-3′; *PSMB3*, 5′-TTCAGCGTCCTGGTGGTGAT-3′ and 5′-ACAGAGCCTGTCATTGCTGG-3′; *PSMB5*, 5′-GCTGGCTAACATGGTGTATCAT-3′ and 5′-AAGTCAGCTCATTGTCACTGG-3′; *PSMB6*, 5′-GAGGGCAGGTGTACTCTGTT-3′ and 5′-CAAAACACCTGCCGCTCTA-3′; *PSMB8*, 5′-ATGATGCTGCAGTACCGG-3′ and 5′-CCGTCTTCCTTCATGTG-3′; *PSMC1*, 5′-GTCACAGTGATGAAGGTGGA-3′ and 5′-ACTTTCATTCTGCGTTCCCG-3′; *PSMC3*, 5′-CAAACGCTTCGACAGTGA-3′ and 5′-CTGGGCTCCATTGAAGTC-3′; *PSMD14*, 5′-TATCAACACTCAGCAGAGCT-3′ and 5′-AATCCTTCCATCCAACTCT-3′.

Preparation of tissue homogenates and immunoblot analysis of proteasome subunits. Livers were homogenized with a Dounce homogenizer in buffer containing 50 mM Tris-HCl (pH 7.8), 200 mM KCl, 5 mM $MgCl_2$, and 1 mM dithiothreitol and centrifuged at 9,000 × *g* for 15 min at 4°C. Protein concentration was determined by the bicinchoninic acid assay (Pierce Inc., Rockford, Ill.), and tissue homogenates were loaded on a sodium dodecyl sulfate-polyacrylamide gel and separated by electrophoresis. Gels were transferred to nitrocellulose membranes (Amersham Pharmacia Biotech Inc., Piscataway, N.J.) at 50 V for 3 h, and immunoblotting was carried out with antibodies against PSMA1, PSMB5, and PSMC1 (Research Diagnostics, Inc., Flanders, N.J.). Immunoblotted membranes were developed by using the ECL Western blotting system (Amersham Pharmacia Biotech Inc.) according to the manufacturer's instructions.

Proteasome activity measurement. Peptidase activity of the proteasome was measured by mixing tissue homogenate with 50 μM fluorogenic peptide Suc-LLVY-AMC (succinyl-Leu-Leu-Val-Tyr-7-amino-4-methylcoumarin), Z-LLB-AMC (Z-Leu-Leu-Glu-7-amino-4-methylcoumarin), or Z-ARR-AMC (Z-Ala-Arg-Arg-7-amino-4-methylcoumarin) (Calbiochem, La Jolla, Calif.) in a final volume of 100 μl. The reaction buffer consisted of 50 mM Tris-HCl (pH 7.8), 20 mM KCl, 5 mM $MgCl_2$, and 1 mM dithiothreitol (36). The mixture was incubated at 37°C for 20 min, and then the reaction was stopped by adding an equal volume of 125 mM sodium borate buffer (pH 9.0) containing 7.5% ethanol. Released fluorogenic AMC was measured at 360-nm excitation and 460-nm emission. Fluorescence units were converted to AMC concentration by using standard curves generated from free AMC.

Plasmids. The promoter region of *PSMB5* (from −3414 to −1; NT 039606) was isolated by PCR amplification from hepatic genomic DNA of ICR mice. The isolated PCR product was ligated into the luciferase reporter vector pGLbasic (Promega, Madison, Wis.). Deleted sequences of the *PSMB5* promoter (−1.1kb-luc, −1080 to −1; −0.5kb-luc, −497 to −1; −0.2kb-luc, −211 to −1) were produced by PCR amplification and inserted into the pGL3 basic vector. Two other truncated promoters [−3.4-del (−1.1)-luc, −3414 to −1079; −0.5kb-del (−0.2)-luc, −497 to −210] were amplified by PCR and ligated into the pGL3 promoter vector, which contains the simian virus 40 promoter as a minimal promoter. Mutated *PSMB5* promoters Mut (−341), Mut (−52), and Mut (−341, −52) were generated by PCR using primers containing the mutated −341 ARE (GCCTGGGCAGTGACCAAAC→GCCTGGGTGGCAACCAAAC) or −52 ARE (TGACGTCGCGGCGTTGCCA→CAACGTCGCGGCGTTGCTG) (mutated nucleotides are underlined) as described previously (26). The sequence of each promoter was verified.

Cell culture and treatment. Embryonic fibroblast cells from 13.5-day-old embryos of mice with wild-type, *nrf2*-disrupted, and *keap1*-disrupted genotypes were immortalized as described previously (44). Cells were maintained in Iscove's modified Dulbecco's media (Life Technologies) containing 10% heat-inactivated fetal bovine serum and antibiotics.

Transient transfection and measurement of luciferase activity. Cells were transfected at 30 to 40% confluence by Lipofectamine Plus reagent (Life Technologies Inc.). Briefly, cells were seeded in 24-well plates at a density of 2×10^4 cells/well. Cells were grown overnight; the transfection complex containing 0.5 μg of plasmid DNA, 0.05 μg of the pRLtk plasmid (Promega), and transfection reagent were added to each well, and cells were incubated for 16 to 18 h. Cells were recovered in normal media after removal of transfection reagents and were then incubated for another 16 to 18 h with or without drug treatment (D3T or sulforaphane). *Renilla* and firefly luciferase activities in cell lysates were measured with the Dual Luciferase assay kit (Promega) with a luminometer (Turner Designs). For overexpression studies, pcDNA3-murine Nrf2 or -murine MafK was cotransfected with promoter plasmids (26).

Chromatin immunoprecipitation assay. Formaldehyde cross-linking and chromatin fragmentation were carried out as described previously (26). Ten percent of the diluted chromatin solution was reserved as the total input of chromatin. The remaining diluted chromatin solution was incubated with an anti-Nrf2 antibody, an anti GATA-1 antibody (Santa Cruz Biotechnology, Santa Cruz, Calif.), nonspecific immunoglobulin G, or no antibody for 18 h at 4°C with rotation. After washing and elution, precipitated DNA was resuspended with 30 μl of water, and 1 μl of DNA was used for 30 to 35 cycles of PCR amplification with the following primers: *PSMB5* −341 ARE (5′-TTGAACCAGGATTAGGATAGGTGG-3′ and 5′-CCATCTTTGAGAAGGGCGTAA-CTG-3′) and *PSMB5* −52 ARE (5′-CAGACCGGCGCTGGTATTTAGAGG-3′ and 5′-TAGCCAGCGCCATGTTTAGCAAGG-3′).

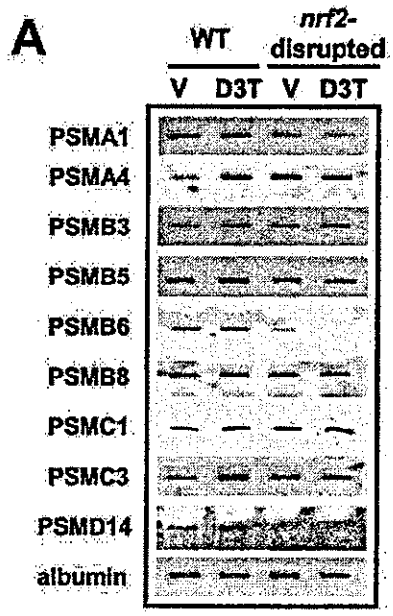

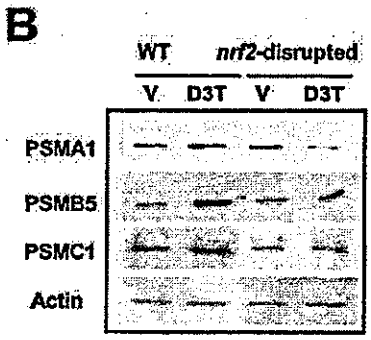

FIG. 2. Induction of 26S transcript and protein levels of subunits by D3T in livers of wild-type mice. (A) mRNA levels for 26S proteasome subunits. Hepatic transcript levels of each subunit in wild-type and *nrf2*-disrupted mice 24 h after treatment with D3T were measured by RT-PCR analysis. Each sample was prepared from three pooled livers. (B) Induction of protein levels for 26S proteasome subunits PSMA1, PMB5, and PSMC1 in wild-type mouse liver by D3T. Immunoblot analyses were performed using subunit-specific antibodies. Each sample was prepared from three pooled livers, and three similar immunoblots were obtained.

RESULTS

Levels of proteasome subunits are increased in mouse liver following treatment with D3T. Microarray analysis indicated that hepatic transcript levels of many proteasome subunits were increased following treatment of mice with D3T (Fig. 1B). Among 36 subunits of the 26S proteasome present on the Affymetrix murine genome U74Av2 GeneChip, levels of 19 subunits were increased by D3T treatment only in wild-type mice, while 5 subunits were induced by D3T treatment in both wild-type and *nrf2*-disrupted mice. Notably, transcript levels of 12 out of 14 subunits of the 20S proteasome catalytic core were increased by D3T treatment. Interestingly, gamma interferon-inducible subunits PSMB8, PSMB9, and PSMB10 were not changed by D3T treatment in either genotype. Induction of these proteasome subunits in livers obtained from vehicle or D3T-treated, wild-type and *nrf2*-disrupted mice was confirmed by RT-PCR analysis (Fig. 2A). Transcript levels of representative subunits of the 20S proteasome, namely, PSMA1, PSMA4, PSMB3, PSMB5, and PSMB6, were elevated two- to threefold 24 h after treatment with D3T in wild-type mice only. A similar pattern of increase was seen for subunits of the 19S proteasome, such as PSMC1, PSMC3, and PSMD14. Levels of proteins PSMA1, PSMB5, and PSMC1 in mouse liver were examined 24 h after treatment with D3T by immunoblot analysis. Polyclonal antibodies for each of these subunits were used for immunoblot analysis, and no nonspecific reactivity was seen. Subunits were detected at 30 (PSMA1), 22 (PSMB5), and 49 kDa (PSMC1). Hepatic levels of the PSMB5 protein were elevated 3.2-fold by D3T treatment compared to those in vehicle-treated wild-type mice, while *nrf2*-disrupted mice did not respond to treatment with D3T (Fig. 2B). Levels of proteins PSMA1 and PSMC1 in wild-type mice were increased 1.9- and 2.3-fold, respectively, following treatment with D3T, but levels in *nrf2*-disrupted mice did not increase. These results indicate that diverse subunits of the 26S proteasome are inducible, largely through a pathway that is dependent on the Nrf2 transcription factor.

Proteasome activities are elevated in D3T-treated mouse liver. Proteasome activity was measured with the fluorogenic peptides *N*-Suc-LLVY-AMC, Z-LLE-AMC, and Z-ARR-AMC as substrates to measure chemotrypsin-like, postglutamic, and trypsin-like peptidase activities, respectively. These peptidase activities could be inhibited more than 90% by the addition of 10 μM MG 132, a proteasome inhibitor (data not shown). Proteasome activity toward *N*-Suc-LLVY-AMC was elevated 2.1-fold in liver homogenates obtained from wild-type mice 24 h after treatment with D3T compared to activity in vehicle-treated controls (Fig. 3A). Smaller, but significant changes were seen with the other substrates (Fig. 3B and C). However, hepatic proteasome activity was not induced by D3T treatment in *nrf2*-disrupted mice.

PSMB5 is regulated by antioxidants and Nrf2 in murine embryonic fibroblasts. Murine embryonic fibroblasts derived from wild-type and *nrf2*-disrupted mice were treated with different phase 2 enzyme inducers to identify the effect of indirect antioxidants on the expression of the proteasome. Levels of mRNA for *PMSB5* were elevated 2.1-fold ($P < 0.05$) by treatment with either D3T or sulforaphane in wild-type fibroblasts (Fig. 4). However, the less potent inducers butylhydroxytoluene and ethoxyquin did not significantly change the level of PSMB5 mRNA. None of the inducers elevated levels of PSMB5 transcripts in *nrf2*-disrupted fibroblasts. To analyze the regulation of *PSMB5*, the promoter region (3.4 kb) was isolated from genomic DNA of mouse liver by PCR amplification and ligated into the luciferase reporter pGL3 basic vector. The murine 20S proteasome subunit β5, *PSMB5*, is located in chromosome 14 and contains several ARE-like motifs in its promoter region. Two tandem AREs were identified 341 and 52 bp upstream of the *PSMB5* gene coding region. The ARE located at the −52 position is a perfect ARE with a sequence of TGACGTCGC, while the ARE at the −341 position is TGACCAAAC, with an AC instead of GC. These candidate